A Binary Scalar Symbolic Field Yields Elementary Particles Consistent With General Relativity

Michael H. Tomasson[1]

[1]Department of Internal Medicine,
University of Iowa,
Iowa City, IA 52242, USA

michael-tomasson@uiowa.edu

July 17, 2025

Abstract

The Standard Model and Quantum Field Theory (QFT) describe the microscopic world with remarkable precision, while General Relativity (GR) provides an apparently accurate account of spacetime and gravity. Yet fundamental gaps remain. These range from the measurement problem to unresolved discrepancies such as the muon $g-2$ anomaly and the vacuum energy density. To address these challenges, we introduce a Symbolic Structure Field Theory (SSFT) rooted in a binary scalar field ψ_0, extended by a local vector field ψ_1 that detects entropy gradients, and a fiber bundle gauge field ψ_2 enabling motif classification and dynamics. Strikingly, 14 unique-under-manifold-roation 8-bit $2\times2\times2$ motifs in ψ_0 yield a clean physical correspondence with the elementary particles of QFT. The framework also encodes geodesic curvature from motif structure, obviating the need for a cosmological constant. Furthermore, it elevates the Hilbert–Pólya Conjecture into a constructive formalism that links a spectral realization of the Riemann Hypothesis to the emergence of physical law. Observables are explicitly defined, enabling empirical validation or falsification.

Comments: 82 pages, 8 figures, 145 equations

Contents

1 Introduction

General Relativity (GR) posits a continuous spacetime fabric, successfully predicting gravitational curvature, acceleration-time relationships, and large-scale dynamics. On the opposite scale, Quantum Field Theory (QFT) describes the microscopic world through quantized fields and particles, forming the Standard Model.

Despite its success, QFT struggles with gravity—the hypothetical graviton remains elusive. String theory, which models particles as vibrating one-dimensional objects in higher dimensions, offers a potential unification framework, though it remains experimentally unverified. In parallel, quantum information theory has restructured physical law around entropy[1], symbolic constraints, and informational limits. Concepts such as decoherence, entanglement, and no-go theorems suggest that it may be information, not geometry or energy, that forms the foundational substrate of physical reality.

The Symbolic Structure Field Theory (SSFT) described below advances this idea: symbolic patterns in a binary scalar field ψ_0 serve as primary entities. Unlike string theory or causal rewrites (e.g., Wolfram Physics), SSFT embeds information into variational structures, deriving geometry and identity from symbolic motifs. This work formalizes a role for information dynamics and symbolic field projections in Hilbert space construction and motif-based particle definitions.

2 Symbolic Motifs and the Binary Field ψ_0

2.1 Core Definitions

SYMBOLIC FIELD THEORY 1 (ψ_0 Field Definitions). *We begin by defining the minimal symbolic apparatus required to formulate a theory of an ontologiclly primary information (symbolic) field (SSFT). These primitives provide the basis for constructing higher-order structures, including motifs, particles, and geometric projections.*

- $\psi_0 : M \to \{-1, +1\}$ — *a binary scalar field defined on a smooth manifold M,*
- $x \in M$ — *a point in the manifold,*

- $\sigma \in \{-1, +1\}^8$ — *a local binary configuration (motif) defined over a* $2 \times 2 \times 2$ *voxel block,*
- $\mathcal{C}_8$ — *the set of canonical 8-bit symbolic motifs, one per equivalence class under cube rotation,*
- $O \subset S_8$ — *the octahedral rotation group (24 elements), acting on* σ *via index permutation.*

DEFINITION 2.1 (Symbolic Structure). Let M be a topological space (e.g., a manifold, lattice, or mesh). A *symbolic structure* on M is a function

$$\psi_0 : M \to \{-1, +1\} \tag{1}$$

assigning to each point $x \in M$ a symbol from a fixed finite alphabet. These symbols are treated as formal labels rather than numeric values, and encode the simplest nontrivial topology-aware structure on M.

DEFINITION 2.2 (Motif). Let ψ_0 be a symbolic structure on M. A *motif* $\sigma \in \{-1, +1\}^8$ is the restriction of ψ_0 to a $2\times2\times2$ voxel neighborhood around a point $x \in M$, i.e.,

$$\sigma = \big(\psi_0(x_1), \ldots, \psi_0(x_8)\big), \tag{2}$$

where $\{x_1, \ldots, x_8\} \subset M$ are the centers of the neighborhood voxels, ordered lexicographically. We refer to σ as the *motif ID*. Motifs represent minimal local symbolic configurations, equivalent to bitstrings, and are indexed by their lex order.

DEFINITION 2.3 (Cube Rotation Group O). Let $O \subset S_8$ denote the subgroup of the symmetric group S_8 corresponding to rigid 3D rotations of the cube. Each element $\pi \in O$ acts on motif σ by permuting its indices: $\pi \cdot \sigma := (\sigma_{\pi^{-1}(0)}, \ldots, \sigma_{\pi^{-1}(7)})$.

DEFINITION 2.4 (Canonical Motif and Rotational Equivalence). Two motifs σ, σ' are rotation-equivalent if there exists $\pi \in O$ such that $\sigma' = \pi \cdot \sigma$. The canonical representative $\hat{\sigma}$ of a motif class is defined as the lexicographically minimal element of its rotation orbit:

$$\hat{\sigma} := \min_{\pi \in O}(\pi \cdot \sigma) \tag{3}$$

The set $\mathcal{C}_8$ consists of one such canonical motif per equivalence class.

AXIOM 1 (Symbolic Foundation). *Let M be a topological space. There exists a function $\psi_0 : M \to \{-1, +1\}$ (Equation 1).*

such that:

1. *$\psi_0(x) \in \{-1, +1\}$ for all $x \in M$.*
2. *The values of ψ_0 are symbolic labels; no additional structure (e.g., metric, energy, probability) is assumed.*
3. *All derived quantities and observables are constructed from finite configurations of ψ_0 and are invariant under diffeomorphisms of M.*
4. *No auxiliary field, embedding, or analog structure underlies ψ_0; it is the minimal primitive of the theory.*

AXIOM 2 (Symbolic Covariance and Invariant Structure). *Let $\psi_0 : M \to \{-1, +1\}$ as above. Then:*

1. *All derived symbolic structures are invariant under diffeomorphisms $\phi : M \to M$.*
2. *For any smooth invertible map ϕ, we have $S[\psi_0] = S[\psi_0 \circ \phi]$, where S is a derived structure.*
3. *Observables depend on motif configuration, not coordinate position.*
4. *Invariance is symbolic (pattern-based), not geometric (metric-based).*

Explanation: Axiom 2 extends general covariance to symbolic fields. Motif identities are preserved under reparametrization. Two fields with the same motif distribution are physically equivalent.

Remark 1 (Symbolic Structure and Geometric Mediation)**.** The field $\psi_0 : M \to \{-1, +1\}$ defines no intrinsic geometry. But the derived fields ψ_1 and ψ_2 inherit structure from local motifs and induce curvature on M.

In particular:

- ψ_1 captures entropy gradients and directional asymmetry,
- ψ_2 registers motif alignment and activation,

- Together, they define a symbolic metric $G_{\mu\nu}$, from which geodesics, curvature, and dynamics follow.

This establishes a direct projection from symbolic structure to emergent geometry.

Axiom 3 (Geometric Emergence from Symbolic Structure)**.** *Let $\psi_0 : M \to \{-1, +1\}$ be the symbolic structure field on a topological space M, and let $\sigma(x) \in \{-1, +1\}^n$ denote the local motif centered at $x \in M$.*

Suppose:

1. *$\psi_1 : M \to \mathbb{R}^d$ is a motif-derived entropy gradient field, constructed from local contrast.*

2. *$\psi_2 : M \to E$ is the activation section, a fiber bundle field encoding motif-level alignment.*

Then there exists a symmetric $(0, 2)$-tensor field $G_{\mu\nu} : M \to \mathbb{R}$, the symbolic metric*, defined pointwise by:*

$$G_{\mu\nu}(x) := \lambda_1 \, \psi_1^{\mu}(x) \, \psi_1^{\nu}(x) - \lambda_2 \, \psi_2(x) \delta_{\mu\nu}, \tag{4}$$

where $\lambda_1, \lambda_2 \in \mathbb{R}_{>0}$ are coupling constants.

This metric satisfies: $G_{\mu\nu}$ is non-degenerate wherever $\psi_1 \neq 0$; the Levi–Civita connection defined by G induces symbolic geodesics; and the curvature tensor $R_{\mu\nu\lambda\kappa}$ is a symbolic invariant derived from the motif distribution of ψ_0.

Interpretation: The symbolic metric is not assumed—it is derived from contrast and activation structure. Geometry emerges from motif patterns. Curvature, distance, and dynamics follow from symbolic form.

2.2 Unique-Under-Rotation Symbolic Motifs

With a motif as a localized binary configuration extracted from the field ψ_0, we performed an initial characterization of 8-bit non-trivial motifs, i.e. binary vectors of length 8—defined over a $2 \times 2 \times 2$ voxel block in the manifold M. Each motif $\sigma \in \{-1, +1\}^8$ represents a finite, minimal symbolic structure, ordered lexicographically according to a fixed labeling of voxel positions. These motifs serve as the fundamental building blocks of symbolic geometry.

Mathematically, there exist 256 potential 8-bit configurations, but much fewer motifs are structurally distinct under rotation; many are equivalent under the symmetries of the cube, including rotation and reflection. We group motifs into equivalence classes under the action of the octahedral rotation group $O \subset S_8$, which includes the 24 rigid symmetries of the cube.

Using Burnside's Lemma, we compute the number of rotationally unique orbits as: equation $|\mathrm{C}_8| = \frac{1}{|G|} \sum_{g \in G} \mathrm{Fix}(g)$ where G is the rotation group and $\mathrm{Fix}(g)$ counts the number of motifs fixed under each group action $g \in G$. This classical group-theoretic approach returns *23 orbits*, each representing a class of 8-bit motifs indistinguishable under cube rotation.

We used computational methods to rotate, characterize, and systematically classify 256 potential 8-bit motifs and discover 14 canonical motifs and 8 "anti-motifs," i.e. motif bitwise inversions, yielding a total canonical motif count of *22 orbits*. These computation results are nearly identical to those calculated using Burnside lemma. The minor discrepancy between Burnside's 23 and our 22 orbits may be explained by the fact that motif classification in SSFT proceeds by symbolic identity, not geometric symmetry alone. The small discrepancy between Burnside's 23 rotation classes and our computational analysis's 22 canonical motifs probably arises because the identity of the SSFT motif incorporates symbolic compressibility, negation invariance, and informational fixity, properties not captured by geometric action alone. In this framework, two motifs may belong to the same rotation orbit but differ in compression structure or entropy signature. Conversely, some rotational orbits may collapse under symbolic equivalence. As a result, the canonical motifs identified here are not merely geometric representatives, but informational species: entities defined by their internal structure and symbolic persistence within the field ψ_0

We summarize the complete set of 14 canonical motifs and their eight antimotifs in Table **??**, along with symmetry-based quantities such as stabilizer size, spin depth, compression branching degree, and symbolic energy $(\psi_1 + \psi_2)$. Most, but not all motifs have an anti-motif (inverted binary values) because some motifs are self-dual, i.e. 6 motifs have anti-motifs that are rotationally equivalent and therefore not unique. These motifs are labeled "SelfAnti" in the Table.

The relationships and patterns among these binary values allow dynamics to develop. With a combination of computational approaches and visual logic, among 256 possible 8-bit arrangements, we identified 8-bit motifs that

were unique under rotation, representing pre-local patterns that are stable across the manifold. These motifs act as ψ_0 fixpoints: discrete configurations that resist drift thereby supporting internal field structure. With entropy as ψ_0's substrate it entersy the physical world begins to take shape. Higher-order fields, metric tensors, and eventually particle identities described below are emergent.

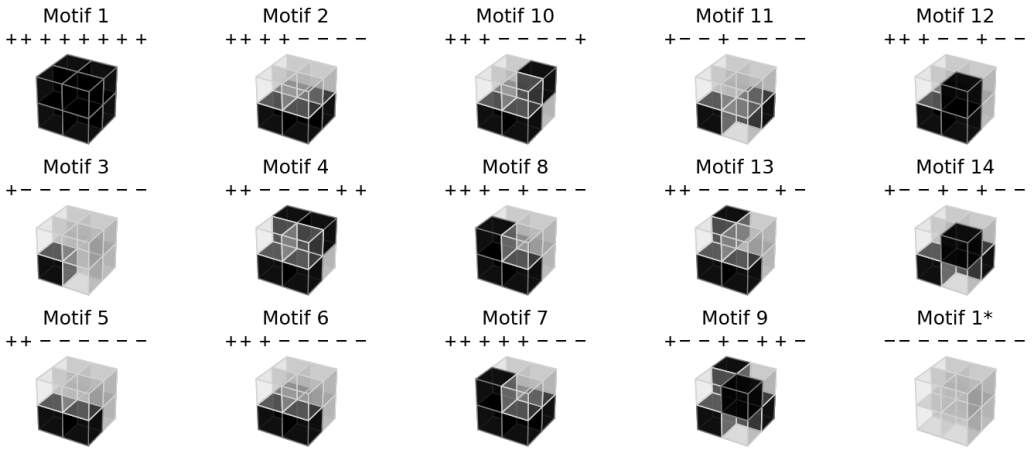

Figure 1: Voxel Plots of Unique 8-bit Motifs. Voxel representations of the 14 unique motifs plus the vacuum motif 1^*, -------- are shown.

Each 8-bit motif under SSTF's formalism possesses internal structure: spin depth, compression branching degree (CBD), entropy, as well as context-dependent attributes, e.g charge. The entropy of a motif measures the number of bit transitions in its voxel pattern. These metrics are not externally imposed nor arbitrary. Motifs inherrently posses directional asymmetry and compressibility. Powerfully, these motifs are field-generating: the properties measured at a motif level admit coherent extension to additional field manifestations over the manifold M.

Motifs with nontrivial spin depth, i.e. low stabilizer size under cube rotation, lack rotational invariance and therefore diplay **directional asymmetry**. These motifs define anisotropic pattern fixpoints and point toward a preferred orientation. Although no absolute coordinate system is defined, ψ_0 can extend motif asymmetry to define ψ_1: a scalar vector field that serves as a kind of entropy compass, and here is where a relative spacetime can

becomes emergent. count of bit-flip boundaries within local motifs. In this sense, ψ_1 inherits its structure directly from motif identity—it measures not geometry, but symbolic curvature arising from contrast. Motifs with high ψ_1 signal structural gradient, symbolic pressure, or internal variation; motifs with $\psi_1 = 0$ act as informational vacua.

2.3 Motif Space is Shared with Anti-motifs

Definition 2.5 (Antimotifs)**.** Given a motif $\sigma \in \mathcal{C}_n$, its symbolic antiparticle is defined as $\bar{\sigma} = -\sigma$, the elementwise negation in $\{-1, +1\}^n$. Since $\psi_2(-\sigma) = \psi_2(\sigma)$, we assign antiparticles to the complementary prime weights:

$$\pi(\bar{\sigma}_i) = p_{(N+1)-i} \tag{5}$$

where $N = |\mathcal{C}_n|$ and primes $\{p_1, \ldots, p_N\}$ are assigned in the canonical ordering.

Proposition 2.6. The pairing $(\sigma, \bar{\sigma})$ forms a symbolic conjugate under ψ_2-invariant negation, with preserved compression and mirrored prime assignment:

$$\psi_2(\bar{\sigma}) = \psi_2(\sigma), \quad \log \pi(\bar{\sigma}) = \log p_{(N+1)-i} \tag{6}$$

Corollary 2.7. The plot of ψ_2 versus $\log p$ for σ and $\bar{\sigma}$ exhibits reflection symmetry about the midpoint of $\log p$, but not in physical space. The motif-antiparticle assignment encodes symbolic charge reversal and topological informational duality.

The choice of the alphabet $\{-1, +1\}$ instead of $\{0, 1\}$ is deliberate. It aligns with the use of signed binary variables in field theory and allows for symmetry under inversion, a useful property for defining antiparticles and curvature dualities. Similarly, we begin with 8-bit motifs, binary configurations defined over a $2 \times 2 \times 2$ voxel neighborhood, because they represent the minimal volumetric unit in a symbolic three-dimensional space. This provides enough structural richness to capture symmetry, contrast, and compression while remaining tractable for classification and enumeration. Below we define the space of canonical 8-bit motifs, which serve as the discrete symbolic particles from which subsequent structures and their properties will be derived.

2.4 Spin Depth via SO(3) Decomposition

Let $\sigma \in \{-1, +1\}^8$ be a binary motif defined over the 8 voxels of a $2 \times 2 \times 2$ cube. Define a mapping $\Phi : \sigma \mapsto f_\sigma \in L^2(\mathbb{S}^2)$ by associating each voxel to a fixed direction (θ_i, ϕ_i) on the sphere:

$$f_\sigma(\theta, \phi) := \sum_{i=1}^{8} \sigma_i \cdot \delta_{(\theta_i, \phi_i)}. \tag{7}$$

Let $\mathcal{H}_\ell \subset L^2(\mathbb{S}^2)$ denote the degree-ℓ irreducible representation of SO(3) spanned by spherical harmonics Y_ℓ^m. Define the orthogonal projection:

$$P_\ell(\sigma) := \text{projection of } f_\sigma \text{ onto } \mathcal{H}_\ell. \tag{8}$$

Define the minimal non-vanishing mode:

$$\ell_{\min}(\sigma) := \min\{\ell \in \mathbb{Z}_{\geq 0} \mid P_\ell(\sigma) \neq 0\}. \tag{9}$$

Definition 2.8 (Minimal Angular Momentum–Motif Asymmetry)**.**

$$\texttt{ssym}_{\mathrm{SO(3)}}(\sigma) := \ell_{\min}(\sigma) \tag{10}$$

This index reflects the minimal angular momentum sector required to express the motif, thus measuring symbolic spin asymmetry via SO(3) representation theory.

2.5 Entropy via Symbolic Laplacian Spectrum

Let $\sigma \in \{-1, +1\}^8$ be a motif defined on the voxel indices $V := \{1, \ldots, 8\}$ of the $2 \times 2 \times 2$ cube.

Construct the undirected graph $G_\sigma = (V, E)$ where:

$$(i, j) \in E \iff \text{voxels } i \text{ and } j \text{ are adjacent in the cube.} \tag{11}$$

Define the signal function $f_\sigma : V \to \mathbb{R}$ by $f_\sigma(i) := \sigma_i$.

Let $L = D - A$ be the graph Laplacian of G_σ, where A is the adjacency matrix and D is the degree matrix.

Definition 2.9 (Motif Entropy)**.**

$$\texttt{entropy}_\Delta(\sigma) := \langle f_\sigma, L f_\sigma \rangle = \sum_{(i,j) \in E} (\sigma_i - \sigma_j)^2 \tag{12}$$

This quantity measures symbolic contrast and curvature of σ over the voxel graph, reflecting internal bit-flip variation in a coordinate-free spectral framework.

2.6 The Principle of Symbolic Identity

Let $\psi_0 : M \to \{-1, +1\}$ be the binary symbolic field defined over a smooth manifold M, and let $\sigma \in C_n$ denote a canonical motif defined as a local restriction of ψ_0 to a neighborhood $U_x \subset M$.

Axiom 4 (Absolute Identity of Motifs)**.** *If two local configurations* $\sigma(x_1), \sigma(x_2) \in C_n$ *satisfy*

$$\sigma(x_1) = \sigma(x_2), \tag{13}$$

then these are not merely similar field values—they are physically, geometrically, and symbolically identical. *The motif* σ *is a nonlocal symbolic entity whose realizations across* M *are multiplicities of a single identity, not distinct elements of the field.*

Interpretation: Motifs in C_n are symbolic forms, Leucippus would recognize them immediately as atoms. They are indivisible Their appearances across the manifold are projections of symbolic identity, not independent events. C_8 are primitive forms, i.e. elementary particles. Elementary particles are not defined by spatiotemporal location, they are non-local the way words have local and non-local (semantic) components; identity is invariant and global. SSFT does not deny the phenomenon termed "entanglement"; in Axiom 4 SSFT renders the word undefined within symbolic ontology. What is often treated as quantum nonseparability is here recast as structural multiplicity without paradox. [1]

Observable physical differences—such as entropy gradients, curvature, or signal activation—arise not from the motif itself, but from surrounding field context: variations in ψ_1 and ψ_2, defined below.

[1] In a 1947 letter to Max Born, Einstein refused to accept entanglement referring to it as spooky action at a distance ('spukhafte Fernwirkung,') and expressed his belief that entanglement was not fundamental but if true emerged due to a fundamental theoretical foundation that quantum mechanics had not yet described. Since 1947, the physics community has forged a strong consensus that Einstein was mistaken. This historical take is that Einstein was wrong because his old fashioned understanding of the universe failed to fully grasp and appreciate the full depth of the New Physics. Axiom 4 proposes that Einstein was in fact correct all along. SSFT asserts the underlying foundation that Einstein may have been alluding to.

2.6.1 Operational Consequence

We retain the form $\psi_0 : M \to \{-1, +1\}$, but reinterpret its role: it is not a scalar field in the conventional sense, but a realization map for symbolic structures.

Define the motif realization set for any $\sigma \in C_n$:

$$\mathcal{R}(\sigma) := \{x \in M \mid \psi_0|_{U_x} = \sigma\}. \tag{14}$$

Then the motif σ is to be understood as a single symbolic object, instantiated multiply across M at each point in $\mathcal{R}(\sigma)$. Identity is not indexical; it is absolute.

2.7 Compatibility with Gödelian Incompleteness

The formalism above is compatible with but is not contained by the Gödelian axiomatic system. The symbolic field $\psi_0 : M \to \{-1, +1\}$ is not defined by rules or inference procedures, but by structural realization. Motif classes $\mathcal{C}_n$, entropy fields ψ_1, and recurrence structures are not constructed from string rewriting or function computation, but from finite symbolic configurations.

Therefore, the incompleteness results of Gödel (1931) and the undecidability results of Turing (1936) do not apply to the foundational layer of SSFT. We prove that the C_8 elemental regime is incomputable. But that *does not mean that computation has no role in SSFT*. We show that with C_{17} motifs, Turing machines emerge from the SSFT foundation. Only following curvature, symbolic drift, and gauge-coupled recurrence are motifs computationally realizable.

Conclusion: SSFT is fully compatible with Gödel. Its pre-computational structure lies outside the scope of incompleteness. Its activation regime inherits Turing limits naturally, but these are not retroactively imposed on the symbolic ontology. Instead, Turing points to where ψ_0 begins to formally compute: with C_{17}.

3 Emergent Fields ψ_1 and ψ_2

Definition 3.1 (Directional Entropy Basis)**.** Let $\Sigma_{\max}$ denote the set of motifs with maximal spin depth and high compression complexity. Then

Symmetry Class	**Orbit Representative $\sigma^{(B)}$**	**Stabilizer Order $\lvert G_{17}(\sigma)\rvert$**	**Preserved Symmetries**	**Notes**
Fully Uniform (+)	$(+1,+1,+1)$	6	D_3^*	Maximal symmetry
Fully Uniform (-)	$(-1,-1,-1)$	6	D_3^*	Same as black
Mirror Type A	$(+1,+1,-1)$	2	Identity, one mirror plane	Reflection across vertex bisector
Mirror Type B	$(+1,-1,-1)$	2	Identity, one mirror plane	Complementary to Type A
Fully Asymmetric	$(+1,-1,+1)$	1	Identity only	No geometric symmetry

Table 1: Symmetry classification of middle-layer configurations $\sigma^{(B)} \in \{\pm 1\}^3$ under the dihedral group D_3. Each class is an orbit; the stabilizer subgroup $G_{17}(\sigma)$ captures preserved symmetries. * 3 rotations, 3 mirrors, identity

$\Sigma_{\max} = \{\sigma_{14}, \sigma_{15}, \sigma_{16}, \sigma_{17}\}$ defines a minimal directional basis for symbolic entropy flow in M, under the symbolic field gradient:

$$\nabla\psi_1(x) = \sum_{i=14}^{17} w_i \cdot \nabla\zeta_i(x), \tag{15}$$

for local weights w_i derived from motif frequency and symmetry breaking.

Interpretation: These four motifs constitute the minimal directional frame over which entropy gradients can be resolved. Each provides a high-curvature signature aligned with local asymmetry. Together, they function as a symbolic compass within the field: a motif-indexed frame for contrast-aligned orientation and curvature analysis.

3.1 Implications of ψ_1

The scalar vector field extension of ψ_0 can be interpreted in a variety of ways, but it may be said to act as a physical compass that points along entropy gradients in ψ_0. If this is a metaphor, then it is more than superficial: there also exists inertia in ψ_1 just as a magnetized needle might. ψ_1 is immediately responsive to local entropy gradients, but has memory of past states. Mathematically, inertia is factored into the measurement of its features (measureables). These features give ψ_1 a unique, particular, and measureable character.

ψ_1 is essentially the representation of mass in SSFT, neither ψ_0 nor ψ_2 (discussed later) has mass. ψ_1's effect on curvature is defined as positive (discussed later), and it resides locally, defining origins of spacetime.

Definition 3.2 (Activation Section ψ_2)**.** Let $\psi_0 : M \to \{-1, +1\}$ be the symbolic structure field over a smooth manifold M, and let $\sigma(x) \in \{-1, +1\}^n$ be the local motif at point $x \in M$.

Define $\psi_2 : M \to E$ as a smooth section of a symbolic fiber bundle $\pi : E \to M$, where the fiber E_x encodes motif activation modes at x. We call ψ_2 the **activation section**.

Interpretation: The field ψ_2 determines when and where motifs within ψ_0 become signal-bearing. It activates under structural thresholds (e.g., entropy gradients, motif alignment) and governs symbolic transport, charge emergence, and curvature smoothing. Unlike ψ_1, which encodes local contrast, ψ_2 defines nonlocal signaling and motif-level persistence across the manifold.

4 Time and Measurement

Schrödinger formalized time within quantum mechanics, introducing the first explicit dynamics in a Hilbert space. Dirac took Schrodinger's equation and coupled the wavefunction to relativistic spacetime, introducing spinor structure and Lorentz invariance. Both frameworks preserve a fundamental asymmetry: an *extrinsic* observer is required to achieve field collapse. The stochastic, non-unitary, and externally defined measurement process remains unresolved at the core of quantum theory.

In contrast, SSFT defines measurement is defined *internally*. Once a threshold is crossed and ψ_2 activates its signaling mode, the field is reconfigured. There is no symmetry between ψ_0 and its time-reverse. The triggering of ψ_2 defines a one-way transformation and there is no going back. The arrow of time is topological and emergent in SSFT.

SSFT replaces the idea that the universe needs to be measured to exist. Instead of waiting for an external observer, ψ_0 measures local structure, curvature, and entropy *internally* via ψ_1 and ψ_2.

5 Motif Classes and Symbolic Particles

5.1 Symbolic Particle Classes P_σ

We define *symbolic particle classes* as recurrence sets of a fixed motif under the compression map. These are not excitations in a continuous field, but symbolic invariants arising from local fixpoint identity.

Definition 5.1 (Symbolic Particle Class)**.** Let $\psi_0 : M \to \{-1, +1\}$ be the binary scalar field over manifold M, and let $\sigma \in \mathcal{C}_8$ be a canonical motif. Define a symbolic compression map $C : U_x \subset M \to \mathcal{C}_8$ that assigns to each neighborhood U_x the canonical motif extracted from the restriction $\psi_0|_{U_x}$.

The **symbolic particle class** associated with motif σ is:

$$P_\sigma := \{x \in M \mid C(\psi_0|_{U_x}) = \sigma\} \tag{16}$$

Each class P_σ is a set of all locations in the manifold where the symbolic field locally compresses to motif σ. These sets are purely symbolic: membership depends on structural identity, not spatial proximity or metric properties.

Interpretation. In SSFT, particles are not quantized excitations but informational invariants. A motif defines a particle only if it recurs with sufficient frequency across the field ψ_0. Local motifs that are isolated or unstable do not define particles. Only those that exhibit global recurrence—informational fixity—acquire symbolic identity.

This reinterprets particle indistinguishability in symbolic terms: particles are identical if and only if their motif form is identical.
These properties are not borrowed from QFT physics, they emerge independently from symbolic structure itself. While speculative assignments to known particles are deferred to later sections, the structural resonance is unmistakable.

5.2 Mapping to the Standard Model (Φ_phys)

ID	Motif	$E(\sigma)$	Entropy	Compactness	Particle Assignment
1	`++++++++`	0.000	0.000	1.000	Photon γ
3	`+-------`	14.206	12.000	0.744	Electron e^-
5	`++------`	19.255	16.000	0.593	Muon μ^-
8	`+++-+---`	20.264	16.000	0.547	Electron Neutrino ν_e
11	`+--+----`	20.372	16.000	0.453	Muon Neutrino ν_μ
14	`+--+-+--`	24.222	20.000	0.492	Strange Quark s
6	`+++-----`	24.902	20.000	0.407	Down Quark d
7	`++++---`	26.151	20.000	0.251	Up Quark u
9	`+--+-++-`	28.745	24.000	0.407	Bottom Quark b
2	`++++----`	30.883	24.000	0.140	Charm Quark c
12	`+++--+--`	30.883	24.000	0.140	Top Quark t
13	`++----+-`	30.973	28.000	0.648	Tau τ^-
4	`++----++`	37.271	32.000	0.341	Z Boson Z^0
10	`+++----+`	38.883	32.000	0.140	W Boson W^+

Table 2: Mapping of SSFT canonical motifs to Standard Model particles based on spectral Hamiltonian energy. Each motif is characterized by total symbolic energy $E(\sigma)$, Laplacian entropy (field curvature), and compressibility. Assignments reflect qualitative alignment with mass hierarchy, decay potential, and field-theoretic stability.

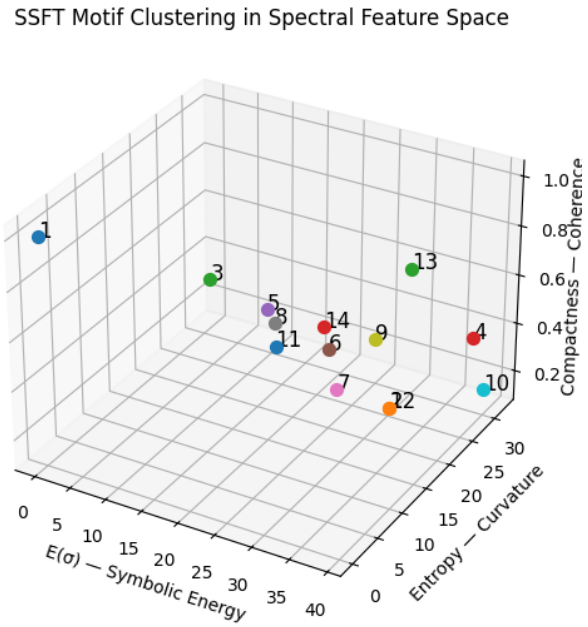

Figure 2: Spectral clustering of SSFT canonical motifs in feature space defined by symbolic energy $E(\sigma)$, Laplacian entropy (curvature), and compressibility. Motifs naturally group into vacuum, lepton-like, quark-like, and bosonic sectors—emerging purely from informational structure.

Table 1 reveals key trends when plotted in parameter space. First, Motif 1, with perfect rotational symmetry, all +1 bits (+) unsurprisingly occupie the lowest energy class (E = 0.00), reflecting minimal structural complexity and maximal stability. As spin asymmetry and bit–flip counts increase, particularly for mid-energy motifs like IDs 3–7, we observe moderate compactness (0.13–0.06), indicating selective persistence in random symbolic environments [2].

Motifs in the 5–7 E-band (IDs 6–9) feature higher BFS and reduced stabilizer symmetry, indicating more complex internal structure. Their compactness spans a wide range, with some showing no stable recurrence (E ≈7.60–7.61) despite similar spin and BFS. The highest energy motif (ID 14) combines maximal BFS (5.0), moderate spin and lower compactness (<0.13), placing it well above simpler structures in the energy hierarchy.

Notably, compactness contributes nontrivially to the energy ordering: motif pairs with identical spin depth and BFS values can be distinguished solely by their compactness values (e.g., IDs 6 and 14 vs. IDs 8 and 12). This validates the inclusion of symbolic persistence as a physically meaningful metric in energy computation.

From these parameters, *parallels between motif identities and QFT particles* begin to emerge unexpectedly. While any mapping of symbolic motifs to QFT particles at thids point is tentative, establishing a parameter-driven assignment provides a useful proof of concept. In **Table 2**, we present an initial mapping of cannonical 8-bit motifs to Standard Model particles. Motifs are grouped according to energy bands in Table 1 and provisionally associated with candidate particle states.

Motif Stratification and Transformability

Motifs in C_8 form the minimal symbolic class: irreducible under motif decomposition. Higher-order motifs (e.g., C_{14}) are composite, capable of transformation, decay, and drift. Identity in SSFT is layered—extending from

[2]Spherical bit arrangements were explored as an alternate motif geometry, but seeking rotational uniformity across a symbolic shell—the cube-based 2×2×2 structure remains canonical. Its discrete symmetries are algebraically rich yet computationally tractable, allowing a full classification of symbolic identities via cube rotations. The cube also defines the minimal symbolic volume that supports three-dimensional contrast and compression. We therefore retain the cube as the elementary motif scaffold, grounding all symmetry, spin, and particle projections in its 8-bit volumetric structure.

structural bit symmetry to topological alignment and dynamic persistence.

5.3 Composite Particles: Tag–Core Formalism

Definition 5.2 (Core–Tag–Tag Motif Decomposition)**.** Let $\sigma_{17} \in \mathcal{C}_{17}$ be a 17-bit symbolic motif. We define a *Core–Tag–Tag decomposition* as a triple:

$$\sigma_{17} = \sigma_c \parallel \tau_1 \parallel \tau_2 \tag{17}$$

where:

- $\sigma_c \in \mathcal{C}_8$ is a canonical core motif embedded in a fixed voxel subregion $V_c \subset \{1, \ldots, 17\}$,
- $\tau_1, \tau_2 \in \{-1, +1\}^6$ are symbolic tag vectors occupying disjoint, non-core voxel subregions V_{t_1}, V_{t_2},
- The regions satisfy $V_c \cap V_{t_i} = \emptyset$, $V_{t_1} \cap V_{t_2} = \emptyset$, and $V_c \cup V_{t_1} \cup V_{t_2} = \{1, \ldots, 17\}$.

Definition 5.3 (Symbolic Decay Functional)**.** Given a C_{17} motif $\sigma_{17} = \sigma_c \| \tau_1 \| \tau_2$, define:

$$\delta(\sigma_{17}) := \alpha\, \psi_1(\tau_1) + \alpha\, \psi_1(\tau_2) + \beta \left| \psi_2(\tau_1) - \psi_2(\tau_2) \right| \tag{18}$$

for fixed $\alpha, \beta \in \mathbb{R}_{>0}$. We say that σ_{17} undergoes symbolic decay if $\delta(\sigma_{17}) > \delta_c$, for a universal threshold $\delta_c \in \mathbb{R}$.

Definition 5.4 (Symbolic Triplet Groupoid)**.** Define a groupoid $\mathcal{G}_3$ with:

- **Objects:** Ordered triplets of canonical motifs:

$$\mathrm{Ob}(\mathcal{G}_3) := \{(\sigma_1, \sigma_2, \sigma_3) \in \mathcal{C}_8^3\} \tag{19}$$

- **Morphisms:** Structure-preserving maps between triplets:

$$\mathrm{Hom}((\sigma_1, \sigma_2, \sigma_3), (\sigma_1', \sigma_2', \sigma_3')) \tag{20}$$

  consists of all permutations $\pi \in S_3$ and tag-induced relabelings such that:

$$\sigma_i' = T_{\pi(i)}(\sigma_{\pi(i)}) \tag{21}$$

  where each T_j is a symbolic morphism (e.g., tag addition, motif inversion, entropy-preserving compression).

Composition is function composition, and identity morphisms are given by the identity permutation with trivial tags.

Definition 5.5 (Fusion Functor to $\mathcal{C}_{17}$)**.** Let $F : \mathcal{G}_3 \to \mathcal{C}_{17}$ be a functor defined as:

$$F(\sigma_1, \sigma_2, \sigma_3) := \mu(\sigma_1, \sigma_2, \sigma_3) \tag{22}$$

where $\mu : \mathcal{C}_8^3 \to \mathcal{C}_{17}$ is a deterministic symbolic fusion map that respects symmetry constraints, compression limits, and total motif entropy bounds.

Morphisms in $\mathcal{G}_3$ are mapped to motif symmetries (e.g., label-preserving voxel automorphisms) in $\mathcal{C}_{17}$.

Definition 5.6 (Symbolic Decay via Inverse Projection)**.** Given a motif $\sigma_{17} \in \mathcal{C}_{17}$, define its preimage orbit:

$$F^{-1}(\sigma_{17}) := \{(\sigma_1, \sigma_2, \sigma_3) \in \mathcal{C}_8^3 \mid \mu(\sigma_1, \sigma_2, \sigma_3) = \sigma_{17}\} \tag{23}$$

Decay corresponds to the selection of a representative in this orbit, via:

$$\text{argmin}_{(\sigma_i) \in F^{-1}(\sigma_{17})} \sum_i E(\sigma_i) \tag{24}$$

Definition 5.7 (Spectral Fingerprint)**.** Let $\sigma \in \mathcal{C}_n$. Define the spectral fingerprint of σ as:

$$\text{Spec}(\sigma) := (\langle \delta_\sigma, \phi_1 \rangle, \langle \delta_\sigma, \phi_2 \rangle, \ldots, \langle \delta_\sigma, \phi_m \rangle) \in \mathbb{R}^m \tag{25}$$

where $\delta_\sigma \in \mathbb{R}^{|\mathcal{C}_n|}$ is the indicator vector of motif σ and $\{\phi_k\}$ are the first m eigenvectors of $\Delta_{\mathcal{C}_n}$.

Definition 5.8 (Spectral Composition Rule)**.** Let $\sigma_1, \sigma_2, \sigma_3 \in \mathcal{C}_8$ and $\sigma_{17} \in \mathcal{C}_{17}$. We say σ_{17} is a spectral fusion of $(\sigma_1, \sigma_2, \sigma_3)$ if:

$$\text{Spec}(\sigma_{17}) \approx \text{Spec}(\sigma_1) + \text{Spec}(\sigma_2) + \text{Spec}(\sigma_3) \tag{26}$$

under an embedding map $\iota : \mathbb{R}^{|\mathcal{C}_8|} \to \mathbb{R}^{|\mathcal{C}_{17}|}$ that aligns Laplacians across motif sizes.

Definition 5.9 (Spectral Decomposition for Decay)**.** Given $\sigma_{17} \in \mathcal{C}_{17}$, find motifs $(\sigma_1, \sigma_2, \sigma_3) \in \mathcal{C}_8^3$ such that:

$$\text{Spec}(\sigma_{17}) \approx \text{Spec}(\sigma_1) + \text{Spec}(\sigma_2) + \text{Spec}(\sigma_3) \tag{27}$$

Decay is the projection:

$$\sigma_{17} \mapsto \text{argmin}_{\{\sigma_i\}} \left\| \text{Spec}(\sigma_{17}) - \sum_{i=1}^{3} \text{Spec}(\sigma_i) \right\| \tag{28}$$

Definition 5.10 (Motif Instantiation Category)**.** Fix $\sigma \in \mathcal{C}_n$. Define the category Mot_σ as:

- **Objects:** Instantiations $x \in M$ such that $\psi_0|_{U_x} = \sigma$.
- **Morphisms:** Diffeomorphisms $\phi : U_x \to U_y$ such that:

$$\psi_0 \circ \phi = \psi_0 \quad \text{and} \quad \psi_2 \circ \phi \simeq \psi_2 \tag{29}$$

  (gauge equivalence).

Composition is composition of diffeomorphisms. Identity morphism is the identity map on U_x.

Definition 5.11 (Triplet Fusion Functor)**.** Define the functor:

$$F : \text{Mot}_{\mathcal{C}_8^3} \to \text{Mot}_{\mathcal{C}_{17}} \tag{30}$$

such that: on **objects**: $(x_1, x_2, x_3) \mapsto x_{17}$ where:

$$\psi_0|_{U_{x_{17}}} := \mu(\psi_0|_{U_{x_1}}, \psi_0|_{U_{x_2}}, \psi_0|_{U_{x_3}}) \tag{31}$$

for a fusion map $\mu : \{-1, +1\}^{8\times 3} \to \{-1, +1\}^{17}$, and on **morphisms**: $(\phi_1, \phi_2, \phi_3) \mapsto \phi_{17}$, where:

$$\phi_{17} := \mu \circ (\phi_1 \times \phi_2 \times \phi_3) \circ \mu^{-1} \tag{32}$$

under symbolic compatibility.

Definition 5.12 (Symbolic Decay via Pullback)**.** Let $x_{17} \in \text{Mot}_{\mathcal{C}_{17}}$. The decay preimage is the fiber:

$$F^{-1}(x_{17}) := \{(x_1, x_2, x_3) \in \text{Mot}_{\mathcal{C}_8^3} \mid F(x_1, x_2, x_3) = x_{17}\} \tag{33}$$

Each triplet represents a possible decomposition of the C_{17} motif identity.

5.4 Embedding $SU(2)$ Doublets via Motif Symmetry

We construct a symbolic analog of the Standard Model weak isospin doublets within SSFT by identifying motif pairs whose internal symmetry structure mirrors $SU(2)$ representations.

5.4.1 Motif Selection for Quark Doublets

From Table 2, we identify two canonical motifs preliminarily associated with the up and down quarks:

$$\sigma_u := (+++----{-}{-}) \quad \text{(Motif ID 6)}$$
$$\sigma_d := (++------{-}{-}) \quad \text{(Motif ID 5)}$$

These motifs differ by a single bit flip and form adjacent points in motif space under the Hamming metric. Their symbolic characteristics from Table 1 are:

Motif	ID	Spin Depth s_{sym}	Bit-Flip Score (BFS)
σ_u	6	4.6	1.0
σ_d	5	3.6	1.0

Both motifs exhibit minimal local entropy (BFS = 1.0), but differ in rotational asymmetry: σ_u has deeper spin symmetry-breaking. This distinction supports their interpretation as an $SU(2)$ doublet—one component more anisotropic, the other more symmetric.

Figure 2, which displays motif-level symbolic charge Q_{sym} under randomized gauge coupling, reinforces this pairing: σ_u and σ_d exhibit small, approximately equal and opposite mean symbolic charges. These charges are not intrinsic, but interaction-induced, highlighting a shared symmetry structure with differential gauge response.

We define the symbolic $SU(2)$ doublet:

$$\Psi_{\text{doublet}} := \begin{pmatrix} \sigma_u \\ \sigma_d \end{pmatrix} \in \text{Motif}^2. \tag{34}$$

5.4.2 Doublet Construction

Definition 5.13. $SU(2)$ doublet We define a symbolic $SU(2)$ doublet as a two-component object in motif space:

$$\Psi_{\text{doublet}} := \begin{pmatrix} \sigma_u \\ \sigma_d \end{pmatrix} \in \text{Motif}^2 \tag{35}$$

This pair admits symbolic $SU(2)$ transformations that act on the symbolic motif doublet basis, with entropy vector gradients ψ_1 distinguishing them under curvature flow. The observed charge asymmetry reflects their role as interaction eigenstates, rather than fixed quantum number carriers in alignment with SSFT's axiomatic structure.

This doublet serves as the symbolic analog of the (u_L, d_L) weak isospin doublet in the Standard Model. The motif pair structure admits a group action by $SU(2)$:

$$\Psi'_{\text{doublet}} = U \cdot \Psi_{\text{doublet}}, \quad U \in SU(2) \tag{36}$$

where the action is formally defined over the vector space spanned by σ_u and σ_d within the symbolic Hilbert space H_Σ.

Interpretation: This pair admits symbolic $SU(2)$ transformations that act on the motif doublet basis, with entropy vector gradients ψ_1 distinguishing them under curvature flow. The observed charge asymmetry reflects their role as interaction eigenstates, rather than fixed quantum number carriers in alignment with SSFT's axiomatic structure. In this setting, the asymmetry between σ_u and σ_d—particularly the difference in spin depth s_{sym}—encodes the symmetry-breaking that differentiates weak isospin components. The $SU(2)$ symmetry acts on the doublet space, while the symbolic fields ψ_1 and ψ_2 induce entropy gradients and compression fields that break this symmetry locally.

5.5 Fractional Charge via Motif Triplet Averaging

SSFT defines charge not as an intrinsic attribute of isolated motifs, but as a contextual observable arising from motif–motif interactions across a symbolic gauge field. This perspective aligns with the relational ontology of SSFT: observables such as symbolic charge emerge through covariant transport and gauge-mediated coupling, not as pre-assigned scalars. In this section, we

demonstrate how composite motif configurations can realize effective fractional charges, consistent with the behavior of quarks in the Standard Model.

5.5.1 Triplet Motif Construction

Let $\sigma_1, \sigma_2, \sigma_3 \in C_8$ be three motifs with symbolic charges $Q^{(i)}_{\text{sym}}$ measured via the gauge field interaction profile as defined by Equation (6). Define the composite symbolic triplet:

$$\Sigma_{\text{triplet}} := \{\sigma_1, \sigma_2, \sigma_3\}, \quad \text{with } Q^{\text{avg}}_{\text{sym}} := \frac{1}{3}\sum_{i=1}^{3} Q^{(i)}_{\text{sym}}. \tag{37}$$

This average defines a motif-cluster-level symbolic charge, modeling the additive field contribution from three co-localized symbolic sources. Because symbolic charge in SSFT arises from differential coupling, such clusters may yield fractional values through structured interactions.

5.5.2 Example: Down-Type Quark Triplet

Suppose the motifs σ_i are selected to have charges:

$$\begin{aligned} Q^{(1)}_{\text{sym}} &= -1, \\ Q^{(2)}_{\text{sym}} &= 0, \\ Q^{(3)}_{\text{sym}} &= 0, \end{aligned}$$

then the resulting composite charge is:

$$Q^{\text{avg}}_{\text{sym}} = \frac{-1+0+0}{3} = -\tfrac{1}{3}. \tag{38}$$

Similarly, an up-type quark could be modeled using two positively coupled motifs and one neutral motif, yielding $+\frac{2}{3}$ symbolic charge.

Interpretation and Emergence: This construction reflects a key feature of SSFT: symbolic charge is an emergent, interaction-based quantity. The triplet motif model does not approximate intrinsic fractional values, but realizes them through the spatial and structural superposition of gauge-coupled motifs. In doing so, it mirrors the phenomenology of QCD, where quarks' individual fractional charges manifest only in confined combinations. SSFT

thus offers a structurally grounded mechanism for fractionalization that arises from informational interaction rather than assigned number.

5.6 Topological Quantization of Symbolic Charge via the First Chern Class

In classical gauge theory, electric charge quantization arises from topological constraints on fiber bundles—particularly through the integrality of characteristic classes such as the first Chern class. SSFT inherits and reinterprets this structure through its symbolic gauge field ψ_2 and connection A_μ, which collectively define a $U(1)$ principal bundle over the motif manifold. Here we show that symbolic charge in SSFT can be quantized via the de Rham cohomology class of the symbolic curvature 2-form, reproducing a quantization condition parallel to Dirac charge quantization in electromagnetism.

5.6.1 Symbolic Curvature and Connection

Let $A_\mu(x)$ be the symbolic connection 1-form, defined via weighted motif mode gradients as in Equation (13), and let the symbolic curvature tensor (field strength) be:

$$F_{\mu\nu}(x) := \partial_\mu A_\nu(x) - \partial_\nu A_\mu(x). \tag{39}$$

This curvature tensor $F_{\mu\nu}$ measures the non-integrability of symbolic motif transport across the manifold M, i.e., the holonomy of symbolic identity under parallel transport.

5.6.2 Definition of the Symbolic First Chern Class

The symbolic analog of the first Chern class is given by:

equation $\mathrm{c}_1^{\mathrm{sym}} := \left[\frac{1}{2\pi}F\right] \in H^2(M;\mathbb{Z})$,

where F is interpreted as a closed differential 2-form over M, and the square brackets denote the cohomology class modulo exact forms. The class c_1^{sym} measures the topological obstruction to globally trivializing the symbolic bundle defined by ψ_2.

5.6.3 Quantization Condition

The total symbolic charge Q_{sym} integrated over a compact 2-cycle $\Sigma \subset M$ satisfies:

$$Q_{\text{sym}} = \int_{\Sigma} \frac{1}{2\pi} F = \int_{\Sigma} c_1^{\text{sym}} \in \mathbb{Z}. \tag{40}$$

This implies that the symbolic charge enclosed by Σ is quantized, regardless of the local motif structure, provided the underlying gauge field configuration is smooth and the bundle is nontrivial.

Interpretation This topological result reveals a second, global mechanism for symbolic charge quantization in SSFT, complementing the local, interaction-driven emergence described in previous sections. Here, quantization is a **consequence of curvature and topology**: the discrete spectrum of Q_{sym} is enforced by the integrality of the symbolic Chern class, independent of dynamic motif interactions.

This formalism aligns with the geometric interpretation of electric charge in gauge theory, and reinforces the notion that symbolic observables in SSFT are governed by both **local relational dynamics** and **global topological invariants**.

6 Hilbert Space $\mathcal{H}_\Sigma$ and Observable Structure

6.1 Mode Functions and Motif Projections

The symbolic mode functions ζ_i associated with each canonical motif $\sigma_i \in \mathcal{C}_8$ allow us to define a motif-resolved subspace of the binary field ψ_0. We now construct a symbolic Hilbert space $\mathcal{H}_\Sigma$ whose elements are motif-mode functions defined over the manifold M, with inner product induced by symbolic support. Unlike traditional Hilbert spaces defined by integration over spatial coordinates, $\mathcal{H}_\Sigma$ is constructed entirely from symbolic content: it is a vector space of symbolic field components indexed by motif identity.

Definition 6.1 (Motif Instantiation Category)**.** Let $\sigma \in \mathcal{C}_n$ be a fixed canonical motif. Define the realization set:

$$\text{Id}[\sigma] := \{x \in M \mid \psi_0|_{U_x} = \sigma\}. \tag{41}$$

Construct a category Mot_σ as follows:

- **Objects:** Points $x \in \mathrm{Id}[\sigma]$,
- **Morphisms:** Diffeomorphisms $\phi : U_x \to U_{x'}$ such that

$$\psi_0 \circ \phi = \psi_0, \quad \psi_2 \circ \phi \simeq \psi_2. \tag{42}$$

Proposition 6.2. Mot_σ forms a category under composition of morphisms, with identity maps.

Corollary 6.3. The symbolic fields ψ_1, ψ_2 define covariant functors:

$$\psi_1, \psi_2 : \mathrm{Mot}_\sigma \to \mathbf{Vect}, \tag{43}$$

mapping each $x \in \mathrm{Id}[\sigma]$ to its local field value and each morphism to the induced field transformation under ϕ.

Definition 6.4 (Symbolic Hilbert Space $\mathcal{H}_\Sigma$)**.** Let $\{\zeta_i\}$ be the symbolic mode functions derived from the binary field ψ_0, each associated to a canonical motif $\sigma_i \in \mathcal{C}_8$. Define the symbolic Hilbert space as:

$$\mathcal{H}_\Sigma := \mathrm{span}\,\{\zeta_i : M \to \{-1, 0, +1\} \mid C(\psi_0|_{U_x}) = \sigma_i\} \tag{44}$$

with inner product defined symbolically by:

$$\langle \zeta_i, \zeta_j \rangle := \sum_{x \in M} \delta_{\sigma_i, \sigma_j(x)} \tag{45}$$

Proposition 6.5 (Orthogonality of Motif Modes)**.** If $\sigma_i \neq \sigma_j$, then the corresponding mode functions are orthogonal:

$$\langle \zeta_i, \zeta_j \rangle = 0 \tag{46}$$

and each ζ_i satisfies:

$$\langle \zeta_i, \zeta_i \rangle = \#P_{\sigma_i} \tag{47}$$

where $\#P_{\sigma_i}$ denotes the number of occurrences of motif σ_i in the manifold.

The symbolic Hilbert space $\mathcal{H}_\Sigma$ provides a mode decomposition of ψ_0 into orthogonal components labeled by motif identity. Each symbolic particle class P_{σ_i} induces a unique direction in $\mathcal{H}_\Sigma$, and the inner product captures motif prevalence across the field. This space sets the stage for defining symbolic observables, projection operators, and eventually a spectral Hamiltonian in the absence of traditional geometry or curvature.

6.2 Projection Operators and Observable Structure

The symbolic Hilbert space $\mathcal{H}_\Sigma$ admits an orthogonal decomposition into subspaces indexed by canonical motifs $\sigma_i \in \mathcal{C}_8$. Each motif defines a distinct informational identity class, and the field ψ_0 may be projected onto these classes using symbolic projection operators.

These operators act not on geometric regions, but on symbolic structure: they isolate the component of ψ_0 corresponding to a given motif, enabling analysis of field composition via motif identity and recurrence. This decomposition is purely algebraic and operates independently of any geometric curvature or dynamical evolution.

Definition 6.6 (Symbolic Projection Operator Π_i)**.** Let $\zeta_i \in \mathcal{H}_\Sigma$ be the mode function associated with motif $\sigma_i \in \mathcal{C}_8$. Define the projection operator $\Pi_i : \mathcal{H}_\Sigma \to \mathcal{H}_\Sigma$ by:

$$\Pi_i(\zeta_j) := \delta_{ij}\zeta_j \tag{48}$$

Each Π_i is idempotent and orthogonal:

$$\Pi_i^2 = \Pi_i, \quad \Pi_i\Pi_j = 0 \text{ for } i \neq j \tag{49}$$

and the collection $\{\Pi_i\}$ forms a complete resolution of the identity:

$$\sum_i \Pi_i = \mathbb{I} \tag{50}$$

We now extend the projection framework to motif-level observables. These observables are functions from motifs to scalars, mapping symbolic identity to compressibility, entropy, or symmetry.

Definition 6.7 (Symbolic Observable Operator $\hat{O}$)**.** Let $O : \mathcal{C}_8 \to \mathbb{R}$ be a symbolic motif-level observable. Define the linear operator $\hat{O} : \mathcal{H}_\Sigma \to \mathcal{H}_\Sigma$ by:

$$\hat{O} := \sum_i O(\sigma_i)\Pi_i \tag{51}$$

This operator acts diagonally on the motif basis:

$$\hat{O}\zeta_i = O(\sigma_i) \cdot \zeta_i \tag{52}$$

Proposition 6.8 (Expectation Value of a Symbolic Observable)**.** Let $\hat{O}$ be a symbolic observable on $\mathcal{H}_\Sigma$. Then its total symbolic expectation value over the field is:

$$\langle \hat{O} \rangle := \sum_i O(\sigma_i) \cdot \|\zeta_i\|^2 \tag{53}$$

This quantity reflects the weighted prevalence of each motif's observable value across the field ψ_0.

Discussion: The projection–observable formalism equips the symbolic field ψ_0 with a native algebraic structure: each motif $\sigma_i \in \mathcal{C}_8$ defines a projection Π_i, and every scalar-valued invariant $O : \mathcal{C}_8 \to \mathbb{R}$ extends to a diagonal operator $\hat{O}$ on $\mathcal{H}_\Sigma$. This induces a complete observable algebra over motif space, *independent of geometry, coordinates, or field dynamics*. Symbolic quantities such as entropy, compression depth, and spin asymmetry are operator-defined and intrinsic to motif identity, not emergent. Expectation values in this algebra register how ψ_0 resolves into persistent, differentiable, and structurally coupled identities across its motif spectrum.

7 Noether's Principle of Conservation

In the Standard Model, conservation laws emerge from continuous symmetries via Noether's Theorem: invariance under time translation implies energy conservation, rotational symmetry implies angular momentum conservation, etc. SSFT agrees that Noether's theorem is extraordinarily useful, even apart from physical symmetries. Noether's formulation is used to define *symbolic diffeomorphisms* as transformations that preserve motif structure, not spacetime geometry.

Axiom 2 asserts that all derived symbolic structures must be invariant under smooth coordinate transformations and motif-class-preserving permutations. This is our analogue to Noether symmetry: conservation arises not from time or space, but from the persistence of symbolic structure under diffeomorphic action.

Symbolic Noether Principle. *If the symbolic field ψ_0 is invariant under a transformation $\phi : M \to M$) such that the identity of the motif is preserved, then the curvature-derived quantities (e.g., the energy of the motif*

$E(\sigma)$, geodesic structure) are conserved along the evolution of the field. Conversely, if motif identity drifts under curvature flow, symbolic energy is not conserved—because the invariant structure itself has changed.

This symbolic reframing allows conservation laws to emerge not from spacetime dynamics, but from informational stability. When motif classes are fixed under symbolic transformations, curvature is stable; when motif configurations reorganize under entropy and compression gradients, symbolic "energy" reassigns itself accordingly.

Definition 7.1 (Symbolic Electric Charge via U(1) Gauge Invariance)**.** Let $\psi_2^{(\mathrm{em})}$ be a section of a principal $U(1)$-bundle $P(U(1), M)$ with local connection A_μ. Under a global $U(1)$ phase rotation,

$$\psi_2^{(\mathrm{em})}(x) \;\mapsto\; e^{i\alpha}\,\psi_2^{(\mathrm{em})}(x), \tag{54}$$

the action $S[\psi_2^{(\mathrm{em})}, A] = \int \mathcal{L}\, d^4x$ remains invariant. By Noether's theorem, this symmetry yields a conserved current

$$J^\mu = \frac{\partial \mathcal{L}}{\partial(\partial_\mu \psi_2^{(\mathrm{em})})}\, i\,\psi_2^{(\mathrm{em})}, \tag{55}$$

with associated symbolic electric charge

$$Q_{\mathrm{sym}} \;=\; \int_\Sigma J^0\, d^3x, \tag{56}$$

where Σ is a spatial slice. This effectively captures particle charge as the generator of U(1) transformations on ψ_2.

Remark 2. This construction focuses on the electromagnetic gauge substructure. In the future, this may be exteded:

$$\psi_2 \;\in\; \Gamma\big(P(G, M)\big), \quad G = U(1) \times SU(2) \times SU(3), \tag{57}$$

allowing symbolic modeling of *weak isospin* and *color charge* via sections $\psi_2^{(\mathrm{weak/strong})} \in \Gamma\big(P(SU(2) \times SU(3), M)\big)$.

7.1 Toward a Symbolic Foundation of Charge

In conventional quantum field theory, electric charge is an intrinsic quantum number assigned to particles and conserved under local $U(1)$ symmetry

transformations. SSFT, by contrast, reconceives charge as an emergent, relational, and topologically grounded phenomenon. This shift reflects a deeper symbolic ontology, in which observable quantities arise from motif identity, activation multiplicity, and structured transport across the symbolic gauge field.

Layer 1: Local Emergence through Motif Coupling

Symbolic charge Q_{sym} arises not from assigned scalar labels, but from motif–motif interactions mediated by the symbolic gauge field ψ_2:

$$Q_{\text{sym}} = \sum_{x \in \Lambda} \text{Im}\left[\bar{\psi}_2(x) \cdot U_x \cdot \psi_2(x + \hat{e}_\mu)\right], \tag{58}$$

This formulation mirrors lattice QED but reinterprets the charge current as a measure of symbolic misalignment—how motif identity differentially evolves under gauge-transport in symbolic space. In this view, charge is a field response to identity transport tension, not a property possessed by a particle.

Layer 2: Composite Fractionalization via Recurrence Clusters

Fractional charges emerge through motif triplets Σ_{triplet} embedded in a shared recurrence envelope $\mathcal{E}_x$. The symbolic current is averaged:

$$Q_{\text{sym}}^{\text{avg}} = \frac{1}{3} \sum_{i=1}^{3} Q_{\text{sym}}^{(i)}, \tag{59}$$

This reflects the non-locality of symbolic charge: motifs themselves are not charged, but charge emerges through coherent structural superposition. This construction parallels the phenomenology of color confinement in QCD, where individual fractional charges are never isolated.

Layer 3: Topological Quantization via Symbolic Cohomology

Global quantization arises from the symbolic first Chern class:

$$c_1^{\text{sym}} := \left[\frac{1}{2\pi} F\right] \in H^2(M; \mathbb{Z}), \quad F_{\mu\nu} = \partial_\mu A_\nu - \partial_\nu A_\mu, \tag{60}$$

The total symbolic charge on a compact 2-surface $\Sigma \subset M$ is quantized:

$$Q_{\text{sym}}(\Sigma) = \int_{\Sigma} c_1^{\text{sym}} \in \mathbb{Z}. \tag{61}$$

This establishes symbolic charge quantization as a topological invariant, rooted in the holonomy of motif identity transport.

7.1.1 Synthesis

Charge in SSFT is not a primitive scalar but a composite invariant arising from: local motif interaction and symbolic misalignment; motif-class activation multiplicity; and global topological obstruction in symbolic gauge transport.

This triadic structure—emergent, relational, and topological—grounds electric charge as a derived quantity. SSFT thereby unifies conservation, quantization, and fractionalization as consequences of its underlying combinatorial field geometry.

8 Activation and Field-Theoretic Regimes

9 Motif Laplacians and the Geometry of Structure

9.1 Covariant Dirichlet Functional and Symbolic Gauge Curvature

To analyze the spectral energy of symbolic fields modulated by gauge activation, we define a covariant Dirichlet functional that captures signal tension and alignment over the motif space $\mathcal{C}_n$. The field $\psi_2 : \mathcal{C}_n \to U(1)$ serves as a local phase-valued section of a principal fiber bundle $P(U(1), \mathcal{C}_n)$, and all motif interaction is mediated through gauge-invariant quantities.

Definition 9.1 (Gauge-Covariant Link Derivative)**.** Let $U_{\sigma_i\sigma_j} := \psi_2(\sigma_i) \cdot \overline{\psi_2(\sigma_j)}$ denote the gauge link phase between motifs σ_i and σ_j. Define the covariant forward difference as:

$$D_{\sigma_i\sigma_j}\psi_2 := \psi_2(\sigma_i) - U_{\sigma_i\sigma_j} \cdot \psi_2(\sigma_j). \tag{62}$$

This operator measures the failure of ψ_2 to remain parallel along the link from σ_j to σ_i, accounting for local gauge rotation.

Definition 9.2 (Gauge-Covariant Dirichlet Energy)**.** Let $W(\sigma_i, \sigma_j)$ be the affinity between motifs defined as in Section A.2. The covariant Dirichlet functional is defined by:

$$\mathcal{L}_{\text{SSFT}}[\psi_2] := \sum_{\sigma_i, \sigma_j \in \mathcal{C}_n} W(\sigma_i, \sigma_j) \cdot \left| D_{\sigma_i \sigma_j} \psi_2 \right|^2 . \tag{63}$$

This functional is gauge-invariant under the transformation:

$$\psi_2(\sigma) \mapsto e^{i\theta(\sigma)} \psi_2(\sigma), \tag{64}$$

with corresponding link update:

$$U_{\sigma_i \sigma_j} \mapsto e^{i(\theta(\sigma_i) - \theta(\sigma_j))} U_{\sigma_i \sigma_j}. \tag{65}$$

This formulation directly parallels lattice gauge theory, where the covariant derivative defines link-based energy across a discrete base space. The energy $\mathcal{L}_{\text{SSFT}}$ measures the global inconsistency of motif signal alignment, and the vanishing of this functional corresponds to covariant constancy of ψ_2 across $\mathcal{C}_n$.

theory 1 (Spectral Trace Decomposition)**.** *Let $\{\lambda_k\}$ be the eigenvalues and $\{v_k\}$ the orthonormal eigenfunctions of the gauge-covariant Laplacian $\Delta_{\mathcal{C}_n}$ defined in A.4. Then:*

$$\mathcal{L}_{SSFT}[\psi_2] = \sum_k \lambda_k \cdot \left| \langle \psi_2, v_k \rangle \right|^2 . \tag{66}$$

Interpretation. The energy of the symbolic gauge field is fully encoded in its projections onto harmonic curvature modes. Each eigenvalue λ_k reflects the cost of activating motif transitions along eigenmode v_k, while the inner products quantify mode participation.

This identity is the symbolic analog of the heat-kernel spectral trace formula in differential geometry, and provides a concrete computational bridge between motif dynamics and spectral arithmetic.

10 Gauge Field Extension ψ_2

Bundle Setup

Let M be a smooth manifold, and let $\psi_0 : M \to \{-1, +1\}$ be the primary binary field. Define local motifs $\sigma(x) \in \{-1, +1\}^8$ as 2×2×2 blocks centered at each point $x \in M$.

We construct a fiber bundle $\pi : E \to M$, where:

- The fiber $\mathcal{F}_x$ encodes the space of symbolic activation profiles $\mathrm{Act}(\sigma(x), \psi_1(x))$,
- The section $\psi_2 : M \to E$ selects at each point a symbolic signal identity structure,
- The total space E encodes all symbolic signaling modes across the manifold.

Definition 10.1 (Symbolic Connection Field $A_\mu(x)$)**.** Let $\zeta_i(x)$ denote the motif mode functions corresponding to high-curvature motifs $\sigma_{14}, \ldots, \sigma_{17}$. Let $\alpha_i(x)$ be motif activation weights derived from symbolic recurrence and curvature features.

Define the symbolic connection 1-form:

$$A_\mu(x) := \sum_{i=14}^{17} \alpha_i(x)\, \partial_\mu \zeta_i(x) \tag{67}$$

This field encodes the infinitesimal transport structure of motif identity and governs symbolic drift under local translation.

Definition 10.2 (Covariant Derivative of ψ_2)**.** Let $\phi(x)$ be a symbolic field valued in the motif fiber. Define the symbolic covariant derivative:

$$D_\mu \phi(x) := \partial_\mu \phi(x) + igA_\mu(x) \cdot \phi(x) \tag{68}$$

where $g \in \mathbb{R}$ is a symbolic coupling constant. This derivative transports symbolic identity in a curvature-sensitive frame.

Definition 10.3 (Symbolic Field Strength)**.** The symbolic field strength tensor (curvature 2-form) is given by:

$$F_{\mu\nu}(x) := \partial_\mu A_\nu(x) - \partial_\nu A_\mu(x) \tag{69}$$

This tensor measures the non-commutativity of symbolic motif transport, encoding motif-level deformation under closed path propagation.

Definition 10.4 (Symbolic Gauge Transformation)**.** Let $\theta : M \to \mathbb{R}$ be a symbolic phase field. Under local gauge transformation:

$$\psi_2(x) \mapsto e^{i\theta(x)}\psi_2(x), \tag{70}$$

the connection transforms as:

$$A_\mu(x) \mapsto A_\mu(x) - \frac{1}{g}\partial_\mu\theta(x), \tag{71}$$

preserving the covariant derivative:

$$D_\mu\psi_2(x) \mapsto e^{i\theta(x)}D_\mu\psi_2(x). \tag{72}$$

Interpretation: The symbolic gauge structure enables covariant transport, curvature, and topological characterization of signalable motif identity. The section field ψ_2 governs when motifs act; the connection A_μ governs how motif identity is preserved or transformed in transit; and the field strength $F_{\mu\nu}$ encodes symbolic resistance to trivialization. This geometric machinery establishes SSFT as a symbolic gauge theory.

10.0.1 U(1) Gauge Symmetry on the Lattice and Symbolic Charge

We adopt a lattice formulation whereby $\psi_2^{(\mathrm{em})}$ lives at each site n of a symbolic spacetime grid, and transforms under a global U(1) phase:

$$\psi_{2,n} \;\mapsto\; e^{i\alpha}\,\psi_{2,n}, \tag{73}$$

leaving the lattice action $S = \sum_n \mathcal{L}_n$ invariant. Gauge invariance on a discrete lattice is well established in lattice-gauge theory, and discrete-time quantum walks exhibit exact U(1) symmetry and conserved currents in this setting.

By applying a discrete version of Noether's procedure, we define the lattice current J_n^μ on links between sites as:

$$J_n^\mu \;=\; \frac{\partial\mathcal{L}_n}{\partial\psi_{2,n+\hat{\mu}}}\, i\,\psi_{2,n+\hat{\mu}} \;+\; \text{c.c.}, \tag{74}$$

where $\hat{\mu}$ is the unit displacement in the μ-direction. The resulting continuity equation

$$\Delta_\mu^- J_n^\mu = 0 \tag{75}$$

(with Δ_μ^- the backward difference operator) enforces local symbolic charge conservation.

The total symbolic electric charge contained in a spatial slice Σ is thus:

$$Q_{\text{sym}} \;=\; \sum_{n\in\Sigma} J_n^0, \tag{76}$$

which yields integer or fractional values (e.g. ± 1, $\pm 1/3$, $\pm 2/3$) depending on the motif embedding and its coupling to $\psi_2^{(\text{em})}$.

This discrete framework enables direct computation of symbolic charge via simulation: by evolving ψ_2 on a motif-filled lattice under a U(1)-invariant Lagrangian, one can measure J_n^0 and accumulate Q_{sym} for each motif.

In future work, we can extend this construction to non-Abelian substructures:

$$\psi_2^{(\text{weak/strong})} \;\in\; \Gamma\big(P(SU(2)\times SU(3), M)\big), \tag{77}$$

allowing analogous definitions of symbolic weak isospin and color charge via discrete conserved currents.

10.0.2 Setup for Symbolic Charge Computation

In preparation for numerical evaluation of symbolic charge, we embed each motif into the center of a $4 \times 4 \times 4$ voxel lattice. Exterior lattice links are initialized with *random U(1) phases*, i.e.

$$U_\mu(n) = e^{i\theta_\mu(n)}, \quad \theta_\mu(n) \sim \text{Uniform}(0, 2\pi), \tag{78}$$

to simulate a generic gauge-field environment without bias.

Inside the motif region—defined as the central $2 \times 2 \times 2$ subcube—we adopt a controlled phase offset strategy (Option 2): the modulus of ψ_2 is uniformly set to 1 across all sites, while each motif-voxel is assigned a fixed phase $\psi_{2,n} = e^{i\phi_0}$, with $\phi_0 \neq 0$ chosen (e.g. $\pi/2$). This localized phase difference provides a clear perturbation that allows gauge-invariant current J_n^0 to accumulate around the motif core, making Q_{sym} robustly measurable. Exterior lattice sites retain $\psi_{2,n} = 1$.

This hybrid initialization balances two goals: it supports statistically meaningful charge measurements in a noisy gauge background (via random links), while ensuring the motif region carries a well-defined, interpretable gauge-phase perturbation for charge extraction.

With these preparations—random link fields, phase-offset motif embedding, and trivial boundary profiles—we are poised to implement the discrete Lagrangian of Eq. (**??**), compute the lattice current via Eq. (74), and evaluate $Q_{\text{sym}} = \sum_{n\in\Sigma} J^0_n$. The result will offer numerical charge assignments (e.g. ± 1, $\pm 1/3$), providing the first empirical test of symbolic charge emergence for our canonical motifs.

10.1 Charge Calculation via Gauge Interaction Profiles

In canonical gauge theory, electric charge emerges from the structure of a local $U(1)$ symmetry: it is the conserved quantity associated with phase-invariant covariant transport. The physical current is defined through

$$J^\mu = \text{Im}(\bar{\psi} D^\mu \psi), \tag{79}$$

and total charge arises from integrating this current across spacetime. This construction is not empirical—it is mathematical: an expression of how local symmetries constrain field interaction.

In SSFT, we adopt the same maths, with essentially no modifications. SSFT's gauge field ψ_2 is defined as a section over a $U(1)$ bundle, and its coupling to randomized gauge connections U_x allows us to define charge through covariant transport across the lattice.

Definition 10.5 (Charge)**.** Let $\psi_2 : \Lambda \to U(1)$ be a section of the symbolic gauge field over a discrete lattice Λ, and let $U_x \in U(1)$ be the link variable connecting site x to its neighbor in a fixed lattice direction μ. Then the *symbolic charge* associated with a configuration ψ_2 is defined as:

$$Q_{\text{sym}} = \sum_{x\in\Lambda} \text{Im}\left(\bar{\psi}_2(x) \cdot U_x \cdot \psi_2(x + \hat{e}_\mu)\right). \tag{80}$$

This expression is is structurally identical to the charge integral in lattice gauge theory: gauge-invariant under local $U(1)$ transformations and defines a net symbolic current induced across the lattice in direction μ.

We next sought to measure Q_{sym} for each motif in section context. We embedded each of the 22 canonical 2^3 motifs within a symbolic 12^3 lattice and measure the resulting net symbolic current when a second motif was placed adjacent in one of 36 geometrically valid neighbor positions (6 directions $\times$ 6 orientations). Each pairing was repeated 10 times with fresh random gauge fields to average over background fluctuations.

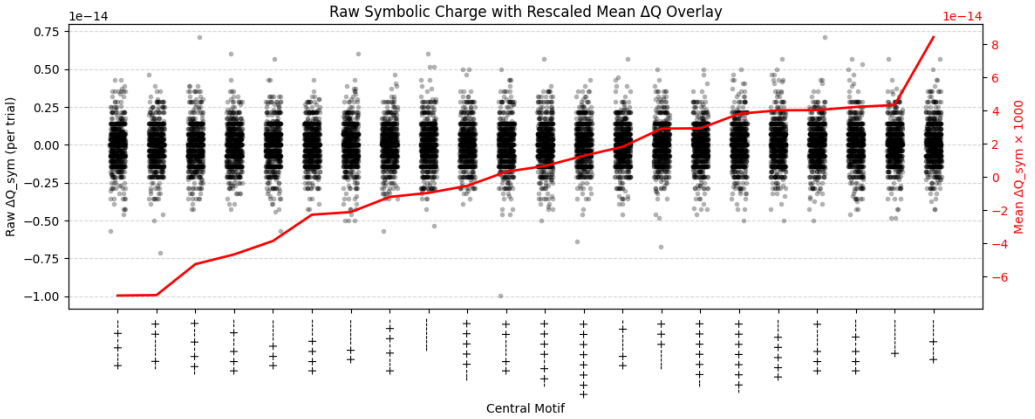

Figure 3: Raw Charge Q_{sym} Values and Mean Q_{sym} for Each Motif. Raw data generated by calculating Q_{sym} for each motif, with scale on the left. Charge values for each motif are unimorphic around 0.0. Mean Q_{sym} is over- layed as a red line, with the scale on the right.

The heatmap of motif charges (Figure 5) is well structured, not a noise field nor a monotonic energy ladder. Rather, this matrix makes it self-evident that charge is not a scalar property of a motif but a function defined through its differential coupling to others. Each motif has a unique interaction signature: some are donors, others absorbers; some are locally inert, others geometrically expressive.

The implications are structural. Charge is not viewed as a label assigned to particles. SSFT does not assign charge charge is generated. That is, charge is an intrinsic response arising from gauge structure itself. The same maths used to define charge in QFT, i.e. covariant transport, gauge invariance, and Noether symmetry, in SSFT yield charge without metaphor or approximation.

Symbolic charge Q_sym is not a toy model or pedagogical scaffold. *It is charge*, defined and measurable in a purely symbolic field. And if symbolic charge exists in this setting, then so too do the principles of energy, field interaction, and symmetry-breaking, not as analogues, but as foundations. SSFT argues that electromagnetism was always a projection of deeper structure.

11 Gauge Field ψ_2: Activation and Dynamics

Definition 11.1 (Symbolic Euler–Lagrange Equation)**.** Let $\psi_2 : M \to E$ be a section of a symbolic fiber bundle with covariant derivative $D_\mu \psi_2$, and let $\mathcal{L}_{\psi_2}$ be the symbolic Lagrangian density:

$$\mathcal{L}_{\psi_2}(x) := \langle D_\mu \psi_2, D^\mu \psi_2 \rangle - V(\psi_2) - \frac{1}{4} \operatorname{Tr}(F_{\mu\nu} F^{\mu\nu}). \tag{81}$$

Then the symbolic Euler–Lagrange equation is:

$$\frac{\delta \mathcal{L}_{\psi_2}}{\delta \psi_2} - D_\mu \left(\frac{\delta \mathcal{L}_{\psi_2}}{\delta D_\mu \psi_2} \right) = 0. \tag{82}$$

11.1 Expanded Field Equation

In local coordinates and under the inner product structure on fibers, this becomes:

$$D^\mu D_\mu \psi_2 + \frac{\delta V}{\delta \psi_2} = 0, \tag{83}$$

where: $D^\mu D_\mu \psi_2$ is the symbolic Laplacian (covariant); and $\delta V / \delta \psi_2$ is the symbolic gradient of the potential energy functional.

Interpretation: This equation describes the dynamics of the symbolic signal field ψ_2 in the presence of motif structure, entropy gradient, and symbolic curvature. It governs how signal identities persist, collapse, or propagate under motif-level constraints and field-level structure. The term $D^\mu D_\mu \psi_2$ encodes signal tension and transport, while $\delta V / \delta \psi_2$ encodes symbolic inertia and resistance to overactivation.

11.2 Symbolic Potential Energy for ψ_2

Definition 11.2 (Symbolic Potential Energy $V(\psi_2)$)**.** Let $\psi_2 : M \to E$ be a section field evaluating symbolic activation over motif structures $\sigma(x) \in \{-1, +1\}^8$. Define the local motif entropy as $\psi_1(\sigma(x))$, and let $\mathrm{CBD}(\sigma(x)) \in \mathbb{N}$ be the Compression Branching Degree of the motif.

We define the symbolic potential energy as a motif-evaluated scalar functional:

$$V(\psi_2(x)) := f\big(\psi_1(\sigma(x)),\, \mathrm{CBD}(\sigma(x))\big), \tag{84}$$

where $f : \mathbb{R} \times \mathbb{N} \to \mathbb{R}_{\geq 0}$ is a structurally weighted symbolic energy model.

11.3 Re-framing Gauge Fields

In Standard Model QFT, the narrative asserts that local gauge fields arise from the requirement to preserve symmetry under localized transformations. That is, a global symmetry is promoted to a local one, and the resulting loss of invariance is compensated by the introduction of a gauge field $A_\mu(x)$—a connection that restores equivariance under local action.

This canonical view has been mathematically useful and operationally indispensable. From the perspective of SSFT however, framing gauge theory as a required fix to preserve symmetry reverses the structural causality. SSFT proposes the opposite: it is not the demand for symmetry that gives rise to the gauge field, but the presence of a structured, irreducible *asymmetry*. Directional motifs, those exhibiting maximal internal spin depth and compression complexity, produce nondeformable anisotropies across the manifold. To compare such structures between locations, a directional field becomes *necessary*. The symbolic gauge field does not exist in SSFT to preserve symmetry but as a way to interpret symbolic asymmetry across spacetime.

SSFT's perspective shifts the explanatory role of gauge fields from compensatory mechanisms to geometric extensions. In this reframing, local symmetry is not the origin but the consequence: it is the apparent residual structure that emerges when directional motifs are globally interpreted through a shared field. The gauge field does not protect symmetry; it makes symmetry interpretable in a world constituted by asymmetry.

11.4 Activation and Structural Context

While identity is invariant, physical effects may differ across instantiations due to field-theoretic context.

Definition 11.3 (active realization set)**.** of a motif σ as:

$$\mathcal{A}[\sigma] := \{x \in \mathrm{Id}[\sigma] \mid \psi_2(x) \neq 0\}\,. \tag{85}$$

This set identifies locations where the motif σ participates in symbolic signaling or transport.

We may further classify motif behavior by local symbolic curvature. Define the cohomology class of symbolic curvature associated to σ at x as:

$$[F]_\sigma(x) := [F_{\mu\nu}(x)] \in H^2(M;\mathbb{R}). \tag{86}$$

Two instantiations $x_1, x_2 \in \mathrm{Id}[\sigma]$ are said to be *curvature-coherent* if:

$$[F]_\sigma(x_1) = [F]_\sigma(x_2). \tag{87}$$

Interpretation: This reformulation eliminates the need for symbolic recurrence envelopes or motif neighborhoods. Instead, identity arises directly from symbolic form. The manifold M serves only to locate instantiations, not to confer identity. Physical variation across realizations is governed not by structure but by context: activation via ψ_2, curvature via $F_{\mu\nu}$, and interaction via ψ_1 gradients. Motifs are primitive; geometry is projected.

11.5 Covariant Derivative of ψ_2

To define variation of the symbolic signal field ψ_2 across the manifold M, we equip the bundle $\pi : E \to M$ with a connection. The connection is determined by the symbolic directional field $A_\mu(x)$, a 1-form derived from the distribution of high-curvature motifs and their gradient-aligned activations. This field arises from weighted derivatives of motif mode functions, and defines a symbolic parallel transport rule.

Given a local trivialization of E, the covariant derivative of ψ_2 is written as

$$D_\mu \psi_2(x) := \partial_\mu \psi_2(x) + igA_\mu(x)\psi_2(x), \tag{88}$$

where $g \in \mathbb{R}$ is a symbolic coupling constant controlling the influence of motif curvature on signal transport. The field A_μ determines how symbolic identity frames shift under infinitesimal displacement, and the derivative $D_\mu\psi_2$ evaluates how signification changes relative to that frame. This expression is structurally identical to a gauge-covariant derivative in a principal bundle setting, though the content of ψ_2 is non-numeric and governed by motif classification and recurrence rather than field amplitude.

The covariant derivative governs the symbolic propagation of motif identity through structured space. When $D_\mu\psi_2 = 0$, the symbolic identity defined by ψ_2 is parallel transported along the direction ∂_μ, maintaining recognition structure across the manifold. When the derivative is nonzero, the identity frame shifts, and motifs may cross activation thresholds or become unrecognizable under symbolic deformation. The field $D_\mu\psi_2$ therefore acts as a local measure of symbolic transition under curvature and identity drift.

Definition 11.4. Curvature term: global symbolic frustration from motif

non-commutativity. The Lagrangian is not fundamental, but the emergent total cost of informational structure.

12 Covariant Symbolic Geodesic Equation

12.1 Geodesic with Symbolic Gauge Coupling

Let $G_{\mu\nu}(x)$ be the symbolic metric tensor defined by motif tension and compressibility fields:

$$G_{\mu\nu}(x) = \lambda_1 \psi_1^{\mu}(x)\psi_1^{\nu}(x) - \lambda_2 \psi_2(x)\delta_{\mu\nu}, \tag{89}$$

and let $A_\mu(x)$ be the symbolic connection 1-form associated with motif transport, with curvature $F_{\mu\nu} = \partial_\mu A_\nu - \partial_\nu A_\mu$.

Let $x^\mu(\tau)$ describe a symbolic trajectory parameterized by symbolic time τ, and let $q \in \mathbb{R}$ denote a symbolic motif charge (curvature coupling constant).

Definition 12.1 (Covariant Symbolic Geodesic Equation)**.** The geodesic trajectory satisfies:

$$\frac{d^2x^\mu}{d\tau^2} + \Gamma^{\mu}_{\alpha\beta}(x)\frac{dx^\alpha}{d\tau}\frac{dx^\beta}{d\tau} = qG^{\mu\nu}(x)F_{\nu\rho}(x)\frac{dx^\rho}{d\tau}, \tag{90}$$

where $\Gamma^{\mu}_{\alpha\beta}$ is the Christoffel symbol derived from $G_{\mu\nu}$, and the right-hand side represents the symbolic analog of a Lorentz-type force: motif drift under gauge-induced curvature.

Interpretation: The geodesic equation encodes symbolic drift under curvature. Local gradients in ψ_1 and ψ_2 define inertial structure. Gauge curvature $F_{\mu\nu}$ induces deflection. Motif identity is transported covariantly: deviation signals field tension, not force.

13 Extension to General Relativity

The symbolic direction field $\mathcal{A}_\mu(x)$ arises not from imposed symmetry but from motif-level asymmetry, i.e. the directional signatures of high-entropy, spin-rich motifs. Its antisymmetric derivative $\mathcal{F}_{\mu\nu}(x)$ defines localized curvature: informational torsion driven by variations in motif activation. This

curvature corresponds to positive mass-like behavior, analogous to gravitational attraction in general relativity.

SSFT contains a second field: $\psi_2(x)$, the activation section. While $\psi_1(x)$ encodes local contrast and entropy gradients, $\psi_2(x)$ activates under structural thresholds and governs symbolic transport. Distributed instances of low-entropy motifs induce curvature smoothing through ψ_2, producing a repulsive effect. This dual structure mirrors the interplay between mass and vacuum energy: ψ_1 concentrates symbolic curvature locally, while ψ_2 distributes it nonlocally via gauge activation.

We now construct the symbolic metric $G_{\mu\nu}(x)$ from ψ_1 and ψ_2. This metric defines geodesics, induces curvature, and satisfies a symbolic analog of Einstein's field equations. Where general relativity relates curvature to energy and momentum, SSFT relates it to motif structure and activation dynamics.

13.1 The SSFT Metric Tensor

In differential geometry, the metric tensor $g_{\mu\nu}(x)$ defines local inner products, geodesic distances, and the curvature of spacetime. Here, we construct an analogous structure: a symbolic metric $G_{\mu\nu}(x)$ built from the fields $\psi_1(x)$ and $\psi_2(x)$. These extensions of ψ_0 encode symbolic tension and compressibility, respectively.

Definition 13.1 (Symbolic Metric Tensor $G_{\mu\nu}(x)$)**.** Let $\psi_1^\mu(x)$ be the directional components of the symbolic tension field $\psi_1(x)$, derived from contrast gradients at the motif level. Let $\psi_2(x)$ be the activation section. Then the **symbolic metric tensor** is defined as:

$$G_{\mu\nu}(x) := \lambda_1 \psi_1^\mu(x)\psi_1^\nu(x) - \lambda_2 \psi_2(x)\delta_{\mu\nu}, \tag{91}$$

where: $\lambda_1, \lambda_2 \in \mathbb{R}^+$ are symbolic coupling parameters; $\delta_{\mu\nu}$ is the Kronecker delta; and $\psi_1^\mu(x)$ denotes the vectorized components of contrast flow.

Interpretation: The first term generates localized, directional curvature from motif asymmetry, analogous to the attractive curvature induced by mass in general relativity. The second term introduces isotropic smoothing via ψ_2, representing the expansive influence of structurally aligned motif regions. The metric $G_{\mu\nu}(x)$ encodes the interplay of symbolic tension and distributed activation.

13.2 Symbolic Geodesics

Given the symbolic metric tensor $G_{\mu\nu}(x)$, we now define the natural trajectories—geodesics—traced by motifs or higher-order symbolic structures as they evolve across the manifold M. These paths represent drift lines in symbolic space, shaped not by physical force but by internal informational curvature.

Definition 13.2 (Symbolic Geodesic Equation)**.** Let $x^\mu(\tau)$ be a motif trajectory parameterized by symbolic time τ. The **symbolic geodesic equation** is:

$$\frac{d^2x^\mu}{d\tau^2} + \Gamma^\mu_{\alpha\beta}(x)\frac{dx^\alpha}{d\tau}\frac{dx^\beta}{d\tau} = 0, \tag{92}$$

where $\Gamma^\mu_{\alpha\beta}(x)$ is the symbolic Christoffel symbol associated with the metric $G_{\mu\nu}(x)$:

$$\Gamma^\mu_{\alpha\beta}(x) := \frac{1}{2}G^{\mu\lambda}(x)\left(\partial_\alpha G_{\beta\lambda}(x) + \partial_\beta G_{\alpha\lambda}(x) - \partial_\lambda G_{\alpha\beta}(x)\right). \tag{93}$$

Interpretation: The symbolic geodesic equation describes how motifs move under the combined influence of local contrast gradients (ψ_1) and global compressibility patterns (ψ_2). It models motif propagation as curvature-aligned drift, where alignment is defined not by energy or velocity, but by informational dynamics.

Figure 5 illustrates a simulated geodesic path traced by a pointlike motif within a symbolic manifold curved by the combined influence of the fields ψ_1 and ψ_2. The trajectory evolves according to the symbolic geodesic equation derived from the informational metric $G_{\mu\nu}(x)$, where local symbolic tension ψ_1 induces curvature and attraction, and symbolic compression ψ_2 induces expansive, repulsive curvature. This balance shapes the motif's path through informational space—not by mass or charge, but by structural asymmetry and symbolic dynamics.

The curve reflects the interplay between two symbolic forces: the attraction toward low-entropy, motif-rich regions (encoded by ψ_1 gradients), and repulsion from zones of maximal compressibility (encoded by ψ_2). This structure mirrors the Einstein field equations of General Relativity [11, 12, 13], where curvature arises from local energy density. The result is a naturally curved path, demonstrating that even in a non-physical manifold, structural motifs generate effective forces and trajectories via informational gradients. This confirms Proposition 3.15: directional motif recurrence, asymmetry, and

compression together induce symbolic curvature, and geodesic drift follows naturally from the informational structure of the field.

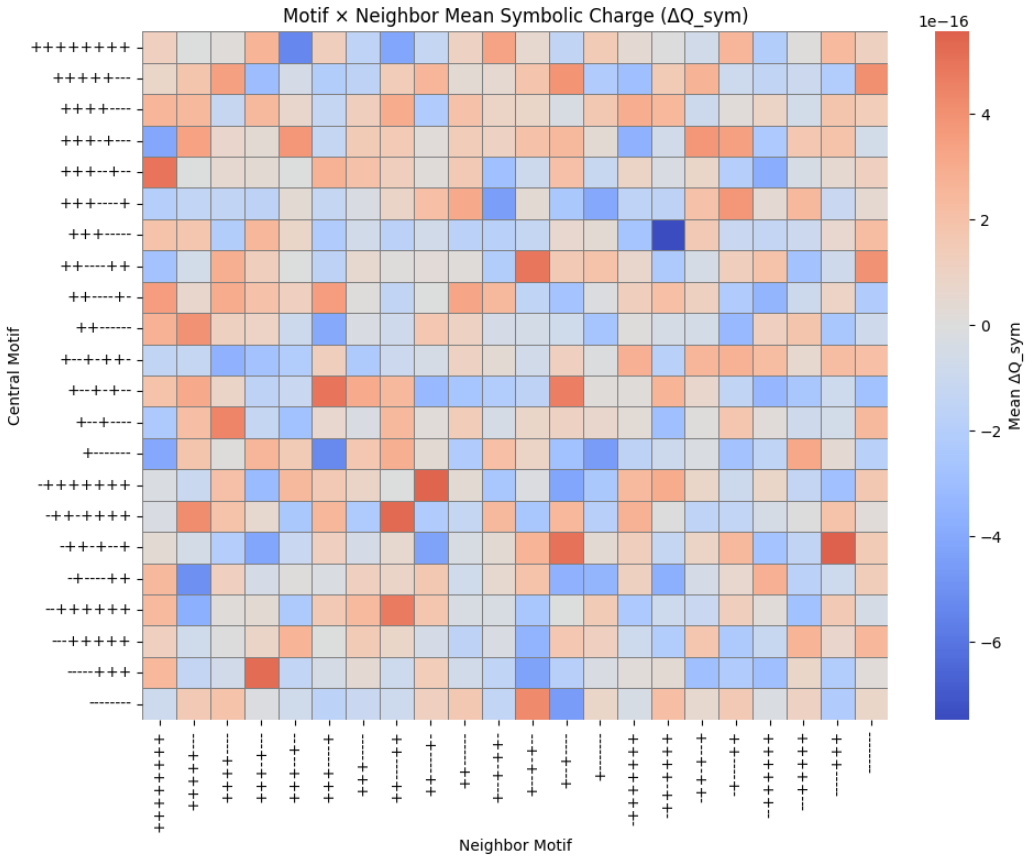

Figure 4: Motif–Neighbor Charge Matrix. The symbolic charge ΔQ_{sym} is measured for all 22 central motifs (rows) paired with each neighbor motif (columns). Each value is the mean of 360 measurements (36 geometric positions $\times$ 10 randomized symbolic gauge fields). Blue indicates negative symbolic charge induced; red indicates positive. Rows and columns are reordered via hierarchical clustering to reveal structural interaction patterns.

To clarify how the symbolic geodesic manifests in trajectory space, Figure **??** isolates the (x, y) projection of the same geodesic shown in Figure **??**. The motif launches from outside the well, descends into the ψ_1 region of local curvature, and is deflected before emerging onto the flattened ψ_2 background. While the path is visibly curved within the well, the global trajectory exhibits no permanent deflection or asymptotic drift. This behavior confirms that, under the SSFT metric, symbolic curvature exerts real influence on local structure without violating overall symbolic symmetry or introducing preferred directions in the manifold.

This geodesic behavior is derived entirely from symbolic curvature without invoking physical mass, energy, or classical force. The ψ_1 well deforms the symbolic manifold locally, modifying the metric tensor and inducing Christoffel terms in the absence of any potential function. The motif's path responds strictly to this intrinsic symbolic geometry, confirming that SSFT supports emergent trajectories through a purely relational framework. Figure **??** visualizes inertial symbolic flow: the motif drifts not through Newtonian attraction, but through informational deformation encoded in ψ_1 and ψ_2. This formalizes one of SSFT's central claims—that directional motion, apparent force, and even deflection can arise from curvature in symbolic space without requiring energetic terms or external dynamics.

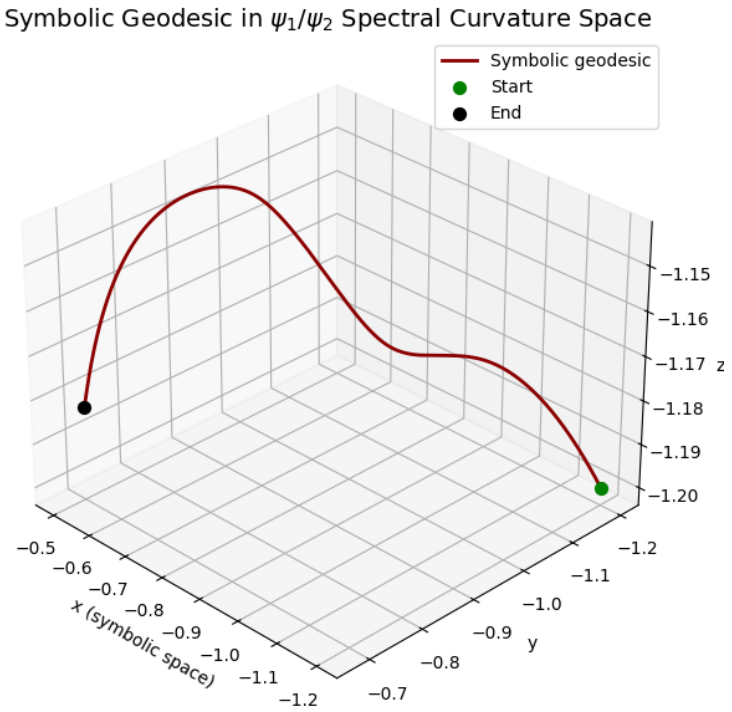

Figure 5: Simulated symbolic geodesic in ψ_1/ψ_2 spectral curvature space. A motif initialized in the curved spectral manifold defined by the entropy mode ψ_1 and the compression mode ψ_2 follows a naturally arcing trajectory. The path bends under symbolic tension (attractive entropy) and is deflected by compression-induced curvature (repulsive compression). The resulting drift confirms Proposition 3.15: symbolic curvature arises from motif asymmetry and compression gradients, and informational geodesics emerge from spectral forces in the symbolic Laplacian.

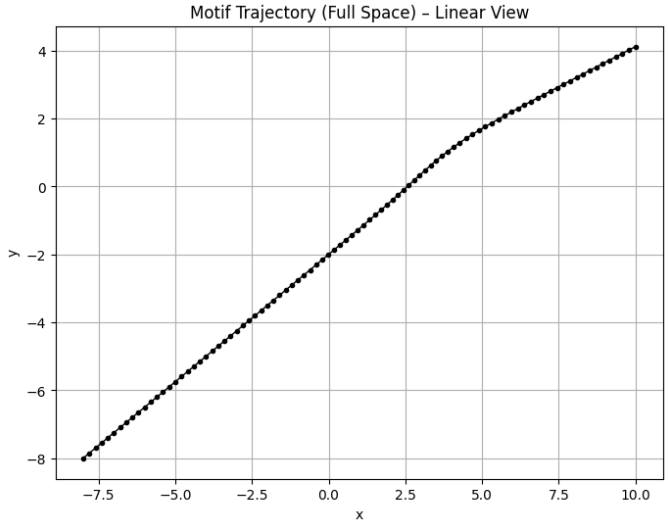

Figure 6: Geodesic trajectory of a symbolic motif evolving in (x, y) space under the SSFT Lagrangian defined by ψ_1 and ψ_2. The smooth path curvature results entirely from the underlying symbolic geometry, with no kinetic or potential energy defined. This demonstrates pure informational motion along a symbolic manifold, with visible curvature emerging from local ψ_1 deformation.

These symbolic geodesics are abstract, but may gain empirical relevance when interpreted through the lens of gravitational phenomena such as black hole mergers, whose informational curvature may be tracked within SSFT's categorical framework.

13.3 Hierarchical Black Hole Mergers as State Morphisms in SSFT

Recent developments in gravitational wave astronomy—most notably event GW231123—present extreme-mass-ratio binary black hole mergers with progenitor masses within the traditional pair-instability mass gap. These events exhibit near-extremal spin and mass growth consistent with multi-generational gravitational collapse. Within the SSFT framework, such phenomena admit a precise categorical interpretation.

Let $\mathcal{O}_{\mathrm{BH}}$ denote the object class of resolved black hole states, each specified by a pair (M, χ) representing ADM mass and dimensionless spin. The process of hierarchical merger is then encoded as a compositional morphism

$$f : \mathcal{O}_{(M_1,\chi_1)} \otimes \mathcal{O}_{(M_2,\chi_2)} \longrightarrow \mathcal{O}_{(M_f,\chi_f)} \tag{94}$$

subject to energy and angular momentum conservation, and regulated by the local geometry of $\mathcal{M}_{\mathrm{gap}} \subset \mathrm{Ob}(\mathcal{C}_{\mathrm{BH}})$—the subcategory of forbidden mass transitions.

This formulation allows for *functorial tracking of state history*: a given black hole remnant $\mathcal{O}_{(M,\chi)}$ retains internal data corresponding to its morphogenetic ancestry, definable in terms of a hierarchical chain

$$\mathcal{H} : \mathcal{O}_0 \longrightarrow \cdots \longrightarrow \mathcal{O}_n = \mathcal{O}_{(M,\chi)}$$

where each transition $\mathcal{O}_i \to \mathcal{O}_{i+1}$ is a merger morphism obeying SSFT dynamical constraints.

In contrast to standard quantum field theory, which lacks the capacity to encode historical morphisms between effective states, SSFT permits this refinement through the enrichment of the black hole category with memory-preserving morphisms. The gravitational wave signal surface Σ_{GW} associated to each merger event furnishes observational data which can be interpreted as cohomological traces on the moduli space of black hole states.

This perspective not only resolves the apparent paradox of mass-gap violations, but also suggests a reinterpretation of spin saturation phenomena as approach to boundary points in the enriched moduli space $\mathcal{K}(\chi) \to 1$. The SSFT machinery thus offers a natural language for modeling both the dynamical and observational structure of black hole evolution.

Having defined symbolic curvature through geodesics in $G_{\mu\nu}$, we turn now to the field equations that govern its generation. Just as Einstein linked spacetime curvature to energy and momentum, SSFT relates symbolic curvature to motif contrast and compression structure. The resulting formulation provides the symbolic analog of Einstein's equations.

13.4 Einstein Equations in SSFT

In general relativity, Einstein's equations equate spacetime curvature to stress-energy content. In SSFT, we propose an analogous structure: a symbolic field equation where curvature is sourced not by matter, but by the internal structural fields $\psi_1(x)$ and $\psi_2(x)$.

Definition 13.3 (Symbolic Einstein Equation)**.** Let $G_{\mu\nu}(x)$ be the symbolic metric. The curvature equation is: equation $\mathrm{R}_{\mu\nu} - \frac{1}{2}G_{\mu\nu}R = T_{\mu\nu}^{\mathrm{SSFT}}$,equation with: equation $\mathrm{T}_{\mu\nu}^{\mathrm{SSFT}} := \alpha\,\psi_1^{\mu}\psi_1^{\nu} + \beta\,\psi_2\,G_{\mu\nu}$.

Interpretation: Symbolic curvature arises from directional tension and field activation. Geometry bends under motif structure; stress-energy is replaced by contrast and alignment.

13.5 Corollary: The Symbolic Vacuum Condition

In classical field theory and general relativity, the vacuum is defined as a state devoid of matter and energy. In SSFT, we define the vacuum symbolically: as a field state with no contrast and no compressibility gradient. That is, the vacuum contains no motif-induced curvature or directional structure—it is symbolically null. Of course, this demands that the vacuum also not contain mass or energy.

Corollary 13.4 (Symbolic Vacuum)**.** If the symbolic tension and activation fields vanish:

$$\psi_1(x) = 0, \quad \psi_2(x) = 0 \quad \text{for all } x \in M, \tag{95}$$

then the symbolic structure tensor vanishes:

$$T_{\mu\nu}^{\mathrm{SSFT}}(x) = 0, \tag{96}$$

and the Einstein equation reduces to:

$$R_{\mu\nu}(x) - \frac{1}{2}G_{\mu\nu}(x)R(x) = 0. \tag{97}$$

Interpretation: The symbolic vacuum is flat: no contrast, no activation, no curvature. It is structurally null, requiring no subtraction or renormalization. *The cosmological constant problem does not arise.*

The preceding curvature equations describe how symbolic structure bends the manifold. We now shift perspective: from how motifs shape space, to how their identity persists across it. This demands a categorical formalism that treats motif instantiations as morphism-tracked entities, allowing identity to be transported, transformed, and preserved under symbolic gauge dynamics.

13.6 Categories of Motif Instantiations

The postulate of absolute identity (Axiom 4) asserts that motif realizations at distinct spacetime points are not multiple symbolic entities, but physical instantiations of a single symbolic form. In this subsection, we formalize this perspective using categorical language, constructing a category whose objects are motif instantiations and whose morphisms reflect physically admissible transformations under the symbolic fields ψ_1 and ψ_2.

Let $\sigma \in C_n$ be a canonical motif. Define the set of all its realized instances in the field ψ_0 as:

$$\mathrm{Id}[\sigma] := \{x \in M \mid \psi_0|_{U_x} = \sigma\}. \tag{98}$$

We now construct a category whose objects are elements of $\mathrm{Id}[\sigma]$, and whose morphisms are diffeomorphisms that preserve symbolic identity and gauge structure.

Definition 13.5 (Motif Instantiation Category)**.** Let $\sigma \in C_n$ be fixed. The category $\mathbf{Mot}_\sigma$ is defined as follows: **Objects:** Elements $x \in \mathrm{Id}[\sigma]$, i.e., locations in M where $\psi_0|_{U_x} = \sigma$; **Morphisms:** For any $x, x' \in \mathrm{Id}[\sigma]$, a morphism $f : x \to x'$ exists if there exists a diffeomorphism

$$\phi : U_x \to U_{x'} \quad \text{such that} \tag{99}$$

$$\psi_0 \circ \phi = \psi_0, \quad \psi_2 \circ \phi \simeq \psi_2, \tag{100}$$

where $\simeq$ denotes gauge equivalence (e.g., up to $U(1)$ phase), and $\phi(U_x) = U_{x'}$.

Proposition 13.6. $\mathbf{Mot}_\sigma$ forms a category. Composition of morphisms is given by composition of diffeomorphisms, and each object $x \in \mathrm{Id}[\sigma]$ admits the identity morphism $\mathrm{id}_x : x \to x$.

Proof. Let $f : x \to x'$ and $g : x' \to x''$ be morphisms induced by diffeomorphisms ϕ_1, ϕ_2 respectively. Then the composition $g \circ f$ is induced by $\phi_2 \circ \phi_1$, which is again a diffeomorphism preserving ψ_0 and ψ_2 up to gauge. Identity morphisms exist trivially by the identity map on each neighborhood. □

Corollary 13.7. The symbolic fields ψ_1 and ψ_2 define covariant functors:

$$\psi_1, \psi_2 : \mathbf{Mot}_\sigma \to \mathbf{Vect}, \tag{101}$$

mapping each object $x \in \mathrm{Id}[\sigma]$ to its local field value and each morphism $f : x \to x'$ to the induced transformation under ϕ.

Interpretation: The category $\mathbf{Mot}_\sigma$ models identity as projection, not multiplicity. Morphisms encode gauge-preserving transport. The functorial action of ψ_1 and ψ_2 defines how symbolic tension and activation propagate over instances of a motif.

This structure provides a precise foundation for studying symbolic drift and gauge dynamics. It supports categorical extension to composite motifs and admits enrichment for tracking homotopy-level motif transport.

Definition 13.8 (Active Realization Set)**.** Let $\sigma \in \mathcal{C}_n$ be a canonical motif. Define the active realization set:

$$A[\sigma] := \{x \in \mathrm{Id}[\sigma] \mid \psi_2(x) \neq 0\}. \tag{102}$$

This identifies locations where σ participates in symbolic signaling.

13.7 Motif Multiplicity Effect

Lemma 13.9 (Motif Multiplicity Induces Curvature)**.** Let $\sigma \in \mathcal{C}_n$ be a canonical motif, and let

$$\mathcal{R}(\sigma) := \{x \in M \mid \psi_0|_{U_x} = \sigma\} \tag{103}$$

be the set of its instantiations in the symbolic field $\psi_0 : M \to \{-1, +1\}$.

Suppose $\#\mathcal{R}(\sigma) > 1$ and the instantiations of σ are spatially nonuniform across M. Then the entropy gradient field $\psi_1 : M \to \mathbb{R}^d$ satisfies

$$\nabla\psi_1(x) \neq 0 \tag{104}$$

on a non-null open set, and the induced symbolic metric

$$G_{\mu\nu}(x) := \lambda_1\psi_1^\mu(x)\psi_1^\nu(x) - \lambda_2\psi_2(x)\delta_{\mu\nu} \tag{105}$$

acquires positive curvature. Ergo, multiplicity of motif identity is not directly encoded in ψ_0, but its effects are formally projected as observable curvature. The gravitational signature of symbolic identity is mediated locally by ψ_1 and nonlocally by ψ_2.

Interpretation: Motifs have local effects, but through multiplicity motifs also have non-local effects. The field ψ_0 does not count or track its repetitions. However, when a motif σ appears in any location without full symmetry, it produces entropy gradients in ψ_1. This gradient bends spacetime.

In SSFT, there is no background geometry. There is only the projection of motif asymmetry. The fields ψ_1 and ψ_2 are the mathematical interface between symbolic structure and both local and nonlocal geometric curvature respectively. Although motif multiplicity can not be confirmed from inside the formalism, it can be measured physically, e.g. by watching light bend.

Corollary 13.10 (Empirical Signature of Motif Multiplicity)**.** Let $\sigma \in \mathcal{C}_n$ be a canonical motif with realization set $\mathcal{R}(\sigma) \subset M$, and suppose the induced entropy gradient field ψ_1 is nontrivial:

$$\nabla \psi_1(x) \neq 0 \quad \text{on some } U \subset M. \tag{106}$$

Then the induced symbolic metric $G_{\mu\nu}(x)$ is curved, and this curvature is, in principle, observable via geodesic deviation. That is:

1. Photons or massless symbolic excitations following null symbolic geodesics

$$\frac{d^2x^\mu}{d\tau^2} + \Gamma^\mu_{\alpha\beta}(x)\frac{dx^\alpha}{d\tau}\frac{dx^\beta}{d\tau} = 0 \tag{107}$$

   will experience nonzero deflection in U;

2. The trajectory of such excitations can be used to infer curvature, and thus nonuniform multiplicity of σ;

3. Conversely, spatial curvature observed empirically via deflection, delay, or geometric deviation is consistent with—and may be entirely attributable to—motif multiplicity in the symbolic field ψ_0.

Interpretation: The multiplicity of the motif is not encoded locally, but its curvature is locally measurable. The symbolic field ψ_0 does not report how often a motif occurs. But the entropy gradients it generates deform the metric. These deformations are visible to any field that propagates via the symbolic geodesic equation. Thus, symbolic multiplicity becomes an empirical observable indirectly through its gravitational shadow.

14 Spectral Modes of ψ_0

Beyond their discrete structural features, e.g. entropy, spin depth, palindromicity, symbolic motifs can also be analyzed through the spectral geometry of their interrelations. By defining a Laplacian operator over the

canonical motif space, we construct a discrete spectral basis for symbolic field variation. Each eigenmode of this operator corresponds to a harmonic of internal structure: the smoothest eigenvectors describe global variation over the motif graph, while higher modes encode increasingly fine-grained oscillations of symbolic tension.

Definition 14.1 (Symbolic Motif Graph and Laplacian Operator)**.** Let $\mathcal{C}_8$ be the set of canonical 8-bit symbolic motifs. Define the **symbolic motif graph** $G = (V, E)$ as: the vertex set $V = \mathcal{C}_8$ consists of all canonical motifs; and an edge $(\sigma_i, \sigma_j) \in E$ exists if σ_i and σ_j differ by a minimal symbolic transformation, such as: a single bit-flip within the 8-bit motif (Hamming distance 1); a change in compression branching degree CBD by ± 1; or a rotation that alters spin depth by the minimal possible increment.
Define the **symbolic Laplacian** operator $\Delta_{\mathcal{C}}$ on G by:

$$\Delta_{\mathcal{C}} := D - A \tag{108}$$

where: A is the adjacency matrix of G, and D is the degree matrix: a diagonal matrix with $D_{ii} = \deg(\sigma_i)$.

Interpretation: The Laplacian $\Delta_{\mathcal{C}}$ encodes the combinatorial geometry of motif space under minimal symbolic deformation. Its spectrum defines a harmonic basis over G: the lowest eigenmodes cluster motifs into structurally coherent regions—motifs with similar compressibility, symmetry, and entropy—while high-frequency modes capture fine-grained contrast, motif instability, and symbolic decay potentials. These eigenmodes define the dynamic architecture of the symbolic field: structure, phase, and evolution are all spectrally embedded.

Figure **??** displays the spectral decomposition of [NEEDS UPDATING:] all 54 canonical motifs (including antimotifs) with respect to the first six eigenmodes of the symbolic Laplacian $\Delta_{\mathcal{C}}$. Each motif is represented as a stacked bar indicating its projection amplitudes onto the eigenmodes ϕ_k.

Clear structure emerges: motifs with low entropy and high symmetry concentrate their spectral weight in the lowest modes. These motifs exhibit minimal curvature tension and align with large-scale structure in motif space. In contrast, motifs projecting strongly onto higher modes—especially ϕ_5 and ϕ_6—show high local contrast and asymmetry. These are dynamically unstable and prone to symbolic drift or decay.

The spectral fingerprint thus provides a multidimensional signature of each motif's structural role: not only its symmetry class but also its dynamical resonance within the symbolic field. These profiles form the basis for future work in motif classification, compression prediction, and curvature-driven phase inference.

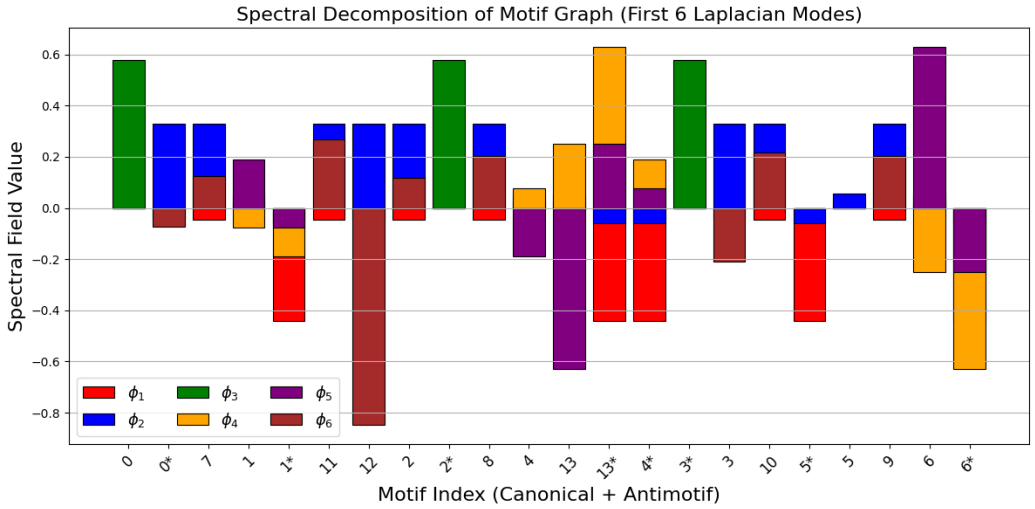

Figure 7: Spectral Decomposition of Canonical Motifs. Each motif (canonical and antimotif) is projected onto the first six eigenmodes $\{\phi_1, \phi_2, \ldots, \phi_6\}$ of the symbolic Laplacian $\Delta_{\mathcal{C}}$ over the motif graph. The stacked bar format reveals each motif's spectral fingerprint: its unique composition in terms of symbolic harmonics. Lower modes (e.g., ϕ_1, ϕ_2) reflect global motif structure and curvature alignment; higher modes (ϕ_5, ϕ_6) emphasize local instability, asymmetry, or entropy gradients. Motifs with smoother harmonic profiles are generally more compressible and stable; those with chaotic or high-frequency structure are more likely to drift or decay under symbolic dynamics.

Analysis of the Laplacian eigenmodes reveals a striking asymmetry between canonical motifs and their antimotifs. While the first three nontrivial modes and the sixth are spectrally balanced across the canonical–antimotif split, Mode 4 concentrates positively on canonical motifs and Mode 5 on antimotifs. This divergence is not imposed by any field-theoretic structure

but emerges intrinsically from the adjacency geometry of the motif graph. Symbolically, this reflects a breakdown of parity invariance: motif–antimotif pairs, though structurally conjugate under negation, do not inhabit equivalent eigenmodes of symbolic variation. We interpret this as a spectral analog of CP asymmetry, an intrinsic geometric separation between matter and antimatter in the symbolic field, without invoking external gauge structure. This spectral fingerprint suggests that charge asymmetry and flavor divergence may arise naturally within SSFT as eigenproperties of the motif Laplacian.

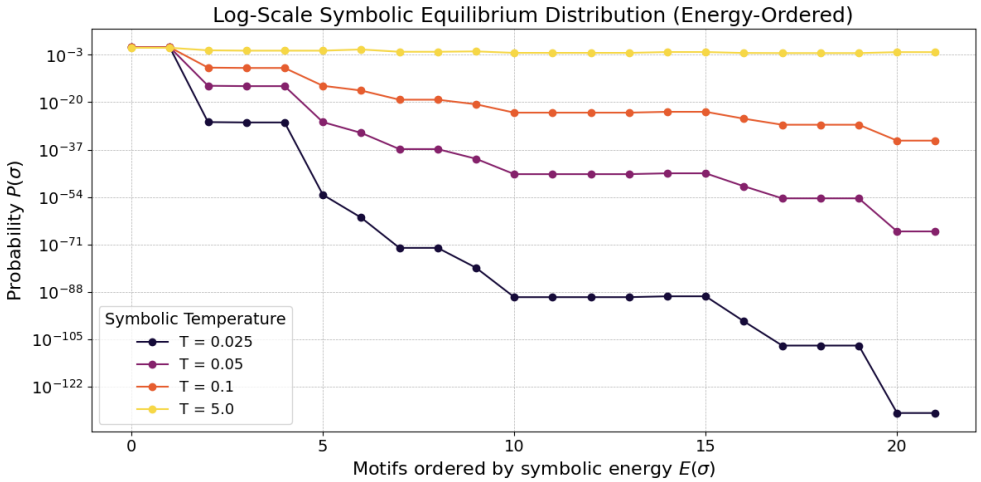

Figure 8: Log-scale symbolic equilibrium distribution over the 22-motif spectrum derived from Table ??, ordered by increasing symbolic energy $E(\sigma) = \psi_1 + \psi_2$. Probabilities $\pi_T(\sigma)$ are computed via the symbolic Boltzmann distribution $\pi_T(\sigma) \propto \exp(-E(\sigma)/T)$, with stabilizer-weighted orbit sizes from Table ??. Lower temperatures yield sharply localized motif populations, while higher temperatures induce symbolic flattening across the energy landscape. Motifs at the left are symbolically minimal (e.g., photon vacuum), while motifs on the right reflect structurally complex, curvature-rich fixpoints.

Proposition 14.2 (Spectral Fingerprint Uniqueness)**.** Let $\Delta_{\mathcal{C}}$ be the symbolic Laplacian defined on the motif graph G over $\mathcal{C}_8$. Let $\{v_k\}$ be the orthonormal eigenvectors of $\Delta_{\mathcal{C}}$.

For each symbolic motif $\sigma_i \in \mathcal{C}_8$, define its spectral fingerprint as the vector of coefficients:

$$\text{Spec}(\sigma_i) := (\langle \delta_i, v_1 \rangle, \langle \delta_i, v_2 \rangle, \ldots, \langle \delta_i, v_m \rangle) \tag{109}$$

where δ_i is the Kronecker basis vector corresponding to motif σ_i. Then $\text{Spec}(\sigma_i)$ is uniquely determined for each σ_i, and no two distinct motifs have identical spectral fingerprints under this basis.

Interpretation: Each symbolic motif has a unique projection onto the spectral basis of $\Delta_{\mathcal{C}}$, defining a harmonic fingerprint that encodes its relational position in motif space. This spectrum captures both geometric curvature and symbolic adjacency, enabling classification beyond symmetry metrics alone.

Figure **??** shows a compositional decomposition of each canonical motif into its projections onto the first six Laplacian eigenmodes. The result is a kind of spectral fingerprint: a stacked bar plot in which each motif is expressed as a weighted sum of symbolic harmonics. These profiles are strikingly diverse and visibly distinguishable, reinforcing that each motif not only carries a unique symmetry class but also a distinct resonance structure within the symbolic field.

This spectral perspective suggests that symbolic motifs, while statically defined by bitstring and symmetry, may also be dynamically decomposed, recomposed, and evolved through their spectral content. A fuller exploration of these harmonic modes—along with the full Laplacian spectrum—is included in Appendix **??**, where we plot the eigenvalues of the symbolic Laplacian and discuss the construction of the motif graph.

Definition 14.3 (Symbolic Temperature Field)**.** Let $\psi_1^\mu(x)$ be the directional entropy field defined from the symbolic field ψ_0. Define the **symbolic temperature** at point $x \in M$ by:

$$T(x) := \sum_\mu |\nabla_\mu \psi_1^\mu(x)| \tag{110}$$

Interpretation: $T(x)$ quantifies the spatial variation of symbolic entropy across all directions. High temperature regions exhibit rapid motif transition, entropy gradients, or symbolic turbulence. Low temperature regions reflect stabilized, coherent motifs. This field governs motif flux and equilibrium in symbolic thermodynamics.

15 Thermodynamics and Phase Transitions

Definition 15.1 (Symbolic Temperature Field)**.** Let $\psi_1^\mu(x)$ be the directional entropy field defined from the symbolic field ψ_0. Define the **symbolic temperature** at point $x \in M$ by:

$$T(x) := \sum_\mu |\nabla_\mu \psi_1^\mu(x)| \tag{111}$$

Interpretation: $T(x)$ quantifies the spatial variation of symbolic entropy across all directions. High temperature regions exhibit rapid motif transition, entropy gradients, or symbolic turbulence. Low temperature regions reflect stabilized, coherent motifs. This field governs motif flux and equilibrium in symbolic thermodynamics.

Definition 15.2 (Symbolic Free Energy)**.** Let $\sigma \in \mathcal{S}$ be a symbolic motif with compression score $\psi_2(\sigma)$ and entropy $\psi_1(\sigma)$. Let $T(x)$ be the local symbolic temperature field.
The symbolic free energy $\mathcal{F}(\sigma)$ is defined as:

$$\mathcal{F}(\sigma) := V(\sigma) - T \cdot \psi_1(\sigma) \tag{112}$$

where $V(\sigma)$ is the symbolic potential energy associated with motif σ, and T is the effective symbolic temperature (locally or globally averaged).

Interpretation: $\mathcal{F}(\sigma)$ quantifies the symbolic cost of maintaining motif σ at a given temperature. Low free energy motifs are structurally stable; high $\mathcal{F}$ motifs are volatile. This function defines motif equilibrium and symbolic selection under thermodynamic constraints.

Definition 15.3 (Symbolic Boltzmann Distribution)**.** Let $\mathcal{F}(\sigma)$ be the symbolic free energy of motif σ, and let T be the global or local symbolic temperature. Then the **equilibrium probability** of motif σ is given by:

$$\pi_{\text{eq}}(\sigma) := \frac{1}{Z} \exp\left(-\frac{\mathcal{F}(\sigma)}{T}\right) \tag{113}$$

where the partition function Z ensures normalization:

$$Z := \sum_{\sigma' \in \mathcal{S}} \exp\left(-\frac{\mathcal{F}(\sigma')}{T}\right) \tag{114}$$

Interpretation: The symbolic Boltzmann distribution defines the long-term motif population in a symbolic environment with fixed temperature. More compressible and less entropic motifs dominate at low T; more disordered motifs persist at high T. This distribution governs symbolic fixpoint selection in thermodynamic equilibrium [6, 7].

Definition 15.4 (Symbolic Entropy Functional)**.** Let $\pi : \mathcal{S} \to [0, 1]$ be a probability distribution over symbolic motifs $\sigma \in \mathcal{S}$, with $\sum_\sigma \pi(\sigma) = 1$.
The symbolic entropy of the motif distribution is defined as:

$$S[\pi] := -\sum_{\sigma \in \mathcal{S}} \pi(\sigma) \log \pi(\sigma) \tag{115}$$

Interpretation: $S[\pi]$ measures the symbolic disorder of a motif population. Higher values indicate greater motif diversity; lower values correspond to dominance by a small number of fixpoints. This entropy governs symbolic thermodynamic evolution and is maximized under equilibrium constraints [6, 7].

Proposition 15.5 (Symbolic Boltzmann Equilibrium)**.** Let $\mathcal{F}(\sigma)$ be the symbolic free energy of motif $\sigma \in \mathcal{S}$, and let T be the symbolic temperature. Then the unique equilibrium motif distribution $\pi_{\text{eq}} : \mathcal{S} \to [0, 1]$ that minimizes free energy and maximizes symbolic entropy is:

$$\pi_{\text{eq}}(\sigma) := \frac{1}{Z} \exp\left(-\frac{\mathcal{F}(\sigma)}{T}\right) \tag{116}$$

with partition function $Z := \sum_{\sigma' \in \mathcal{S}} \exp(-\mathcal{F}(\sigma')/T)$.

Interpretation: In symbolic equilibrium, motif recurrence probabilities follow a Boltzmann-like distribution governed by compression cost, entropy, and symbolic curvature. This distribution is computable from structural motif metrics and enables predictive population modeling in IFT.

Proposition 15.6 (Entropy Maximization at Symbolic Equilibrium)**.** Let $\pi : \mathcal{S} \to [0, 1]$ be a distribution over symbolic motifs with fixed total probability:

$$\sum_{\sigma \in \mathcal{S}} \pi(\sigma) = 1 \tag{117}$$

and fixed expected free energy:

$$\sum_{\sigma \in \mathcal{S}} \pi(\sigma)\, \mathcal{F}(\sigma) = \text{const} \tag{118}$$

Then the unique distribution π^* that maximizes the symbolic entropy functional

$$S[\pi] := -\sum_{\sigma \in \mathcal{S}} \pi(\sigma) \log \pi(\sigma) \tag{119}$$

under these constraints is given by the symbolic Boltzmann distribution:

$$\pi^*(\sigma) = \frac{1}{Z} \exp\left(-\frac{\mathcal{F}(\sigma)}{T}\right) \tag{120}$$

Interpretation: Symbolic fields evolve toward maximal motif diversity under the constraint of fixed structural cost. The resulting motif distribution optimally balances entropy and compression, providing a thermodynamically stable representation of the field's informational structure.

In classical statistical mechanics, a phase transition occurs when a system's macroscopic state changes discontinuously as a function of thermodynamic parameters, typically temperature or pressure. In SSFT, phase transitions are structural: they involve qualitative changes in the motif distribution induced by variations in symbolic temperature $T(x)$ or structural coupling parameters.

Definition 15.7 (Symbolic Phase Transition)**.** Let $\pi_T(\sigma)$ denote the equilibrium motif distribution at symbolic temperature T. A **symbolic phase transition** occurs at temperature T_c if the motif support or dominant motif class changes discontinuously:

$$\lim_{\varepsilon \to 0^+} \pi_{T_c+\varepsilon}(\sigma) \neq \lim_{\varepsilon \to 0^-} \pi_{T_c-\varepsilon}(\sigma) \tag{121}$$

for some $\sigma \in \mathcal{S}$.

Interpretation: A symbolic phase transition marks a qualitative shift in structural stability. For example, at low T, the field may be dominated by uniform motifs (e.g., ID 1 and 26), whereas above T_c, asymmetric or higher-energy motifs may emerge as dominant. The transition may be first-order (discrete motif shift) or second-order (divergent susceptibility in symbolic entropy).

15.1 Probabilities and the Born Rule

In quantum mechanics, the Born Rule defines probability as the square of amplitude: Prob $\sim |\psi|^2$. In information field theory, probabilistic structure arises from symbolic recurrence, compression, and entropy, rather than continuous field amplitudes.

The motif distributions $\pi(n, t)$ are not governed by wavefunction norms but by combinatorial structure: how often motifs appear, how compressible they are, and how they interact with symbolic curvature. In this sense, the Born Rule emerges as a special case where motif modes are orthonormal and symbolically uniform, but IFT defines probability intrinsically through symbolic structure.

Definition 15.8 (Symbolic Motif Distribution)**.** Let $\psi_0 : M \to \{-1, +1\}$ be the symbolic field, and let $\mathcal{C}_n$ denote the set of canonical motifs of size n. Let t be symbolic time (discrete or continuous).

Define $\pi(n, t)$ as the probability that a motif of size n is active in ψ_0 at time t:

$$\pi(n, t) := \text{Prob}(\sigma \in \mathcal{C}_n \text{ occurs in } \psi_0 \text{ at time } t) \tag{122}$$

Interpretation: The function $\pi(n, t)$ defines a symbolic probability distribution over motif sizes. It tracks how fixpoint motifs are distributed by scale and evolves under structural forces such as entropy, compression, and curvature. Motif growth, decay, and stabilization are modeled as shifts in $\pi(n, t)$ over time.

Definition 15.9 (Symbolic Dirichlet Energy Functional)**.** Let $\mathcal{C}_n$ denote the set of canonical symbolic motifs of length n. Let $W : \mathcal{C}_n \times \mathcal{C}_n \to \mathbb{R}_{\geq 0}$ be a symmetric weight function defining edge strengths between motifs in the symbolic motif graph.

Let $\psi_1 : \mathcal{C}_n \to \mathbb{R}$ be a scalar field defined over motifs.
The **symbolic Dirichlet energy functional** is:

$$\mathcal{L}_{\text{IFT}}[\psi_1] := \sum_{\sigma,\tau \in \mathcal{C}_n} W(\sigma, \tau) \left[\psi_1(\sigma) - \psi_1(\tau)\right]^2 \tag{123}$$

Interpretation: This functional quantifies the symbolic tension across motif space. Low values correspond to smooth fields where adjacent motifs carry similar symbolic curvature. The Laplacian operator $\Delta_{\mathcal{C}_n}$ arises as the operator whose eigenvectors minimize $\mathcal{L}_{\text{IFT}}$ under orthogonality constraints.

Definition 15.10 (Symbolic Laplacian Spectrum)**.** Let $\Delta_{\mathcal{C}_n}$ be the symbolic Laplacian operator derived from the motif graph over $\mathcal{C}_n$, as defined by the Dirichlet energy functional $\mathcal{L}_{\text{IFT}}[\psi_1]$.

Then:

- $\Delta_{\mathcal{C}_n}$ is a real, symmetric matrix of dimension $|\mathcal{C}_n| \times |\mathcal{C}_n|$,
- It admits a complete orthonormal basis of eigenvectors $\{v_k\}$,
- The **eigenvalues** λ_k are real and satisfy:

$$0 = \lambda_1 \leq \lambda_2 \leq \cdots \leq \lambda_{|\mathcal{C}_n|} \tag{124}$$

Interpretation: The spectrum $\{\lambda_k\}$ encodes the symbolic curvature and harmonic structure of motif space. Lower eigenvalues correspond to globally coherent variations in ψ_1, while higher modes encode fine-scale symbolic fluctuations. This spectrum forms the foundation for comparisons with physical spectra and number-theoretic eigenvalue distributions.

SYMBOLIC FIELD THEORY 2 (Symbolic Laplacian as Proto-Hilbert–Pólya Operator). *Let $\Delta_{\mathcal{C}_n}$ be the symbolic Laplacian defined over the canonical motif space $\mathcal{C}_n$, derived from the Dirichlet energy functional $\mathcal{L}_{\text{IFT}}[\psi_1]$.*

Then:

1. *$\Delta_{\mathcal{C}_n}$ is real, symmetric, and admits a complete orthonormal eigenbasis,*
2. *Its eigenvalues λ_k reflect the curvature structure of motif space and exhibit statistical regularities resembling Gaussian Unitary Ensemble (GUE) spectra,*
3. *The eigenvectors define symbolic harmonic modes that minimize $\mathcal{L}_{\text{IFT}}[\psi_1]$,*
4. *The spectral structure of $\Delta_{\mathcal{C}_n}$ provides a finite, combinatorial analog of the conjectured Hilbert–Pólya operator $\hat{H}$ satisfying:*

$$\zeta\left(\tfrac{1}{2} + iE_n\right) = 0 \quad \Longleftrightarrow \quad \hat{H}\psi_n = E_n\psi_n \tag{125}$$

Interpretation: SSFT contains a symbolic motif space with curvature, entropy, and symmetry structure. The spectral Laplacian $\Delta_{\mathcal{C}_n}$ encodes tension in this space and may approximate, in the $n \to \infty$ limit, a discrete scaffold for a self-adjoint operator whose spectrum reflects the zeros of the Riemann zeta function. This correspondence opens a path to modeling prime distribution and field identity through a unified spectral geometry.

On the Hilbert–Pólya conjecture, Yakaboylu's 2024 engineered a Hamiltonian whose eigenfunctions satisfy Dirichlet boundary conditions and whose

self-adjoint similarity transform addresses both core stages of the conjecture [**?**]. Bender, Brody, and Müller extended the Berry–Keating xp proposal into a concrete spectral framework, overcoming technical critiques to sustain the vision of a physical operator echoing the zeta spectrum [**?**]. Connes, in a distinct geometric direction, recast prime-counting formulae as spectral trace identities within non-commutative geometry, suggesting that the arithmetic content of RH may be recovered via operator traces over adelic spaces [**?**].

Each of these advances aims to uncover the hidden spectral operator whose *eigenvalues encode the distribution of primes.* SSFT represents a complementary angle: a fully discrete, combinatorially defined Laplacian whose spectrum arises from symmetry, curvature, and entropy among symbolic motifs. The resulting operator $\Delta_{\mathcal{C}_n}$ exhibits real eigenvalues, spectral order, and structural parallels to the conjectured $\hat{H}$—yet remains rooted in physically interpretable field dynamics. This spectral construction parallels the Hilbert–Pólya program, in which an operator encodes the structure of the Riemann zeta function [14, 15, 16]. If the Riemann Hypothesis is a reflection of spectral order in arithmetic space, then SSFT raises the possibility that quantum field spectra, e.g. mass, spin, charge, may be manifestations of the same operatorial logic that governs the primes.

Corollary 15.11 (Arithmetic Spectrum of ψ_2)**.** In light of the spectral structure defined by the symbolic Laplacian Δ_{C_n}, we observe an unexpected arithmetic regularity: motifs with high symbolic compressibility $\psi_2(\sigma)$ correspond monotonically to lower primes when mapped by compression rank. This leads to a corollary of the symbolic Hilbert–Pólya hypothesis: *symbolic motif structure encodes an emergent arithmetic spectrum.*

Let C_n denote the canonical set of n-bit symbolic motifs, with compression score $\psi_2(\sigma)$ and entropy score $\psi_1(\sigma)$ defined as in Sections 3.2 and 3.4. We define a symbolic prime assignment $\pi : C_n \to \mathbb{P}$ such that:

$$\psi_2(\sigma_i) < \psi_2(\sigma_j) \quad \Rightarrow \quad \pi(\sigma_i) < \pi(\sigma_j) \tag{126}$$

Given a motif $\sigma \in C_n$, its symbolic antiparticle is defined as $\bar{\sigma} = -\sigma$, the elementwise negation in $\{-1, +1\}^n$. Since $\psi_2(\bar{\sigma}) = \psi_2(\sigma)$, we assign antiparticles to the complementary prime weights:

$$\pi(\bar{\sigma}_i) = p_{N+1-i} \tag{127}$$

where $N = |C_n|$ and primes $\{p_1, \ldots, p_N\}$ are assigned in the canonical ordering.

Proposition 15.12. The pairing $(\sigma, \bar{\sigma})$ forms a symbolic conjugate under ψ_2-invariant negation, with preserved compression and mirrored prime assignment:

$$\psi_2(\bar{\sigma}) = \psi_2(\sigma), \quad \log \pi(\bar{\sigma}) = \log p_{N+1-i} \tag{128}$$

Corollary 15.13. The plot of ψ_2 versus $\log \pi(\sigma)$ for σ and $\bar{\sigma}$ exhibits reflection symmetry about the midpoint of $\log \pi$, but not in physical space. The motif–antiparticle assignment encodes symbolic charge reversal and topological informational duality.

Interpretation: This structural alignment suggests that ψ_2 acts not merely as a measure of symbolic compressibility, but as a *combinatorial manifestation of number-theoretic order*. The monotonic relation between symbolic order and prime weight implies that internal symmetry—quantified via compression—is arithmetically curved. This arithmetic spectrum is not imposed but emerges intrinsically from the symbolic motif field.

Figure **??** displays this mapping for the 17 canonical motifs and their antiparticles. The plot shows a monotonic alignment: symbolic motifs with lower ψ_2 values cluster toward the high-$\log p$ end (lower primes), while less compressible motifs spread toward lower $\log p$ values. Antiparticles preserve their ψ_2 values but reflect across the axis. This symmetry encodes not just motif pairing, but a topological duality across compression space and prime identity. The appearance of structure in this mapping suggests that motif compressibility may be an emergent arithmetic invariant.

15.2 Definition of the Operator $\hat{H}$

Having defined a symbolic energy functional $E(\sigma)$ over the canonical motif space $\mathcal{C}_8$, we now promote this scalar-valued function to a linear operator acting on the symbolic Hilbert space $\mathcal{H}_\Sigma$. This operator plays the role of a symbolic Hamiltonian. Unlike its physical counterpart, it does not generate time evolution or dynamics in a conventional sense. Instead, $\hat{H}$ provides a spectral ordering of symbolic modes according to intrinsic informational complexity.

Each motif mode function $\zeta_i \in \mathcal{H}_\Sigma$ is an eigenvector of $\hat{H}$, with eigenvalue $E(\sigma_i)$. This induces a discrete symbolic energy spectrum, turning motif identity into an operator-theoretic structure.

Definition 15.14 (Symbolic Hamiltonian Operator $\hat{H}$)**.** Let $\mathcal{H}_\Sigma = \text{span}\{\zeta_i\}$ be the symbolic Hilbert space indexed by canonical motifs $\sigma_i \in \mathcal{C}_8$. Define the symbolic Hamiltonian operator $\hat{H} : \mathcal{H}_\Sigma \to \mathcal{H}_\Sigma$ by:

$$\hat{H}\zeta_i := E(\sigma_i) \cdot \zeta_i \tag{129}$$

where $E(\sigma_i)$ is the symbolic energy of motif σ_i defined via Equation (5.1).

This operator is Hermitian and diagonal in the symbolic motif basis. Its action is purely multiplicative and non-dynamical: each symbolic mode retains its identity under $\hat{H}$, but acquires a spectral weight. As with observables in quantum theory, this operator allows the symbolic field ψ_0 to be decomposed and analyzed according to motif-level energy.

Proposition 15.15 (Spectral Properties of $\hat{H}$)**.** The operator $\hat{H}$ admits a complete orthonormal eigenbasis $\{\zeta_i\}$, with real, nonnegative eigenvalues $E(\sigma_i)$. That is:

$$\mathcal{H}_\Sigma \cong \bigoplus_i \mathbb{C} \cdot \zeta_i, \quad \hat{H}\zeta_i = E(\sigma_i)\zeta_i \tag{130}$$

The symbolic Hamiltonian endows the field ψ_0 with a quantized informational spectrum. This spectrum allows symbolic particles to be ranked, measured, and later thermally populated, all in advance of any geometric curvature or dynamical time evolution. In the next section, we will associate low-energy motifs with elementary particle identities, establishing a symbolic analogy to particle mass.

15.3 Symbolic Compression and Arithmetic Spectrum

We observe a striking correspondence between symbolic compressibility $\psi_2(\sigma)$ and the logarithmic prime weights $\log \pi(\sigma)$ when motifs are ordered by structural simplicity. This emergent relation suggests an arithmetic structure underlying motif space.

Definition 15.16 (Symbolic Prime Assignment)**.** Let $\mathcal{C}_n$ denote the canonical set of n-bit symbolic motifs, ordered by increasing compressibility $\psi_2(\sigma)$. Define a prime assignment $\pi : \mathcal{C}_n \to \mathbb{P}$ such that:

$$\psi_2(\sigma_i) < \psi_2(\sigma_j) \quad \Rightarrow \quad \pi(\sigma_i) < \pi(\sigma_j), \tag{131}$$

assigning smaller primes to more compressible motifs.

Definition 15.17 (Symbolic Antiparticle and Prime Reflection)**.** Given a motif $\sigma \in \mathcal{C}_n$, define its antiparticle as $\bar{\sigma} := -\sigma$, the elementwise negation. Then assign primes to antiparticles by reversed rank:

$$\pi(\bar{\sigma}_i) := p_{N+1-i}, \tag{132}$$

where $N = |\mathcal{C}_n|$ and $\{p_1, \ldots, p_N\}$ are the first N primes in ascending order.

Proposition 15.18 (Prime Symmetry under Compression)**.** The motif–antimotif pair $(\sigma, \bar{\sigma})$ satisfies:

$$\psi_2(\bar{\sigma}) = \psi_2(\sigma), \quad \log \pi(\bar{\sigma}) = \log p_{N+1-i}, \tag{133}$$

i.e., symbolic compressibility is preserved under negation, while prime assignment is reflected.

Corollary 15.19 (Log-Prime Symmetry Curve)**.** The plot of $\psi_2(\sigma)$ versus $\log \pi(\sigma)$ exhibits reflection symmetry for motif–antimotif pairs about the midpoint of $\log p$. This reflects symbolic charge duality, spectral inversion, and informational parity breaking.

Interpretation: The symbolic compression metric ψ_2 correlates with prime-weight ordering in a nontrivial way, suggesting that motifs encode an emergent arithmetic spectrum. The appearance of $\log p$ echoes the structure of spectral traces in analytic number theory and implies that symbolic fixpoint structure may be governed by a deeper arithmetic–informational duality.

16 Hilbert–Pólya Correspondence in SSFT

The Hilbert–Pólya conjecture proposes that the nontrivial zeros of the Riemann zeta function are eigenvalues of a self-adjoint operator on a Hilbert space. In Symbolic Structure Field Theory (SSFT), a Laplacian operator $\Delta_{\mathcal{C}_n}$ arises naturally from motif space $\mathcal{C}_n$, encoding symbolic transitions via entropy and compressibility.

We now construct the spectral framework within which this symbolic Laplacian defines a discrete operator theory analogous to the Hilbert–Pólya conjecture.

16.1 Symbolic Motif Laplacian

Let $\mathcal{C}_n$ denote the set of canonical n-bit symbolic motifs. Define a graph $G = (\mathcal{C}_n, E)$ where edges encode symbolic adjacency (e.g., Hamming distance 1, compression branching transitions).

Definition 16.1 (Symbolic Laplacian)**.** Let A be the adjacency matrix of the motif graph G, and let D be the diagonal degree matrix with $D_{ii} = \deg(\sigma_i)$. The symbolic Laplacian is defined as:

$$\Delta_{\mathcal{C}_n} := D - A \tag{134}$$

The operator $\Delta_{\mathcal{C}_n}$ is real, symmetric, and admits a complete orthonormal eigenbasis $\{v_k\}$ with eigenvalues $\lambda_k \in \mathbb{R}_{\geq 0}$. These eigenmodes define symbolic harmonics over motif space, with λ_k measuring the symbolic curvature or transition tension across motifs.

16.2 Spectral Energy Decomposition

Let $\psi_2 : \mathcal{C}_n \to U(1)$ be the symbolic signal field defined over motif space. We view ψ_2 as a vector in the Hilbert space of motif-valued fields, and expand it in the eigenbasis $\{v_k\}$ of $\Delta_{\mathcal{C}_n}$.

theory 2 (Spectral Trace Decomposition)**.** *Let $\{\lambda_k\}$ be the eigenvalues and $\{v_k\}$ the orthonormal eigenvectors of $\Delta_{\mathcal{C}_n}$. Then the symbolic Dirichlet energy of the signal field ψ_2 is given by:*

$$\mathcal{L}_{SSFT}[\psi_2] = \sum_k \lambda_k \cdot |\langle \psi_2, v_k \rangle|^2 \tag{135}$$

Interpretation: Each term in the sum represents the energetic contribution of eigenmode v_k weighted by its symbolic curvature λ_k. The decomposition quantifies the total symbolic strain across motif space—analogous to a spectral trace in differential geometry.

This identity parallels the heat kernel trace in Riemannian geometry and provides a concrete operator-theoretic framework. In SSFT, symbolic tension is not an imposed structure, but a spectral invariant of motif alignment across the informational manifold.

16.3 Symbolic Compressibility and Arithmetic Spectrum

Let $\psi_2(\sigma)$ denote the symbolic compressibility of motif $\sigma \in \mathcal{C}_n$, computed via harmonic projection onto low-spin spherical modes. Empirically, we observe a monotonic correspondence between $\psi_2(\sigma)$ and $\log p$, where p is the i-th prime in ascending order.

Definition 16.2 (Symbolic Prime Assignment)**.** Let $\mathcal{C}_n = \{\sigma_1, \ldots, \sigma_N\}$ be ordered such that:

$$\psi_2(\sigma_1) < \psi_2(\sigma_2) < \cdots < \psi_2(\sigma_N)$$

Define the symbolic prime assignment:

$$\pi(\sigma_i) := p_i \tag{136}$$

where p_i is the i-th prime number.

Proposition 16.3 (Compression–Prime Reflection)**.** Let $\bar{\sigma}$ denote the antimotif of σ under elementwise negation. Then:

$$\psi_2(\bar{\sigma}) = \psi_2(\sigma), \quad \log \pi(\bar{\sigma}) = \log p_{N+1-i} \tag{137}$$

Hence, the plot of $\psi_2(\sigma)$ versus $\log \pi(\sigma)$ is symmetric about its midpoint.

Interpretation: The field ψ_2 ranks motifs by alignment and structural regularity. When motifs are ordered by ψ_2, their prime assignments exhibit a mirrored spectrum in $\log p$. This pairing suggests an emergent arithmetic structure within symbolic identity.

Motifs and antimotifs thus form spectrally conjugate pairs under symbolic negation, reflecting a deeper arithmetic symmetry embedded within motif space.

16.4 Spectral Operator and Hilbert–Pólya Alignment

Let $\Delta_{\mathcal{C}_n}$ be the symbolic Laplacian on motif space $\mathcal{C}_n$, with spectrum $\{\lambda_k\}$ and eigenfunctions $\{v_k\}$. The symbolic signal field ψ_2 projects into this spectral basis via:

$$\psi_2 = \sum_k \langle \psi_2, v_k \rangle \, v_k$$

This defines a purely combinatorial, self-adjoint operator whose spectrum orders motif transitions by curvature tension—without any reference to energy, mass, or spatial distance.

Definition 16.4 (Symbolic Spectral Operator)**.** Define the operator $\hat{H}_{\text{sym}} : \mathcal{H}_\Sigma \to \mathcal{H}_\Sigma$ by:

$$\hat{H}_{\text{sym}}\, v_k := \lambda_k\, v_k \tag{138}$$

where λ_k are the eigenvalues of $\Delta_{\mathcal{C}_n}$ and $\mathcal{H}_\Sigma$ is the motif Hilbert space spanned by $\{\zeta_i\}$.

The operator $\hat{H}_{\text{sym}}$ is real, symmetric, and discrete, and admits a complete orthonormal basis. Its spectrum encodes the harmonic geometry of symbolic structure over $\mathcal{C}_n$.

Remark 3 (Hilbert–Pólya Correspondence)**.** While we do not assert any formal connection to the nontrivial zeros of the Riemann zeta function, the structure of $\hat{H}_{\text{sym}}$ aligns in form with the conjectured Hilbert–Pólya operator: a self-adjoint linear operator whose eigenvalues mirror the imaginary parts of the zeta zeros.

In particular:

1. The spectrum $\{\lambda_k\}$ is ordered, real, and discrete.
2. The motif ordering induced by $\psi_2(\sigma)$ mirrors the sequence of $\log p$, an arithmetic structure central to explicit formulae in analytic number theory.
3. The spectral trace $\sum_k \lambda_k |\langle \psi_2, v_k \rangle|^2$ mirrors the heat-kernel expansion structure used in zeta function regularization.

These alignments are empirical and structural. No conjecture or inference regarding the Riemann Hypothesis is made. Nevertheless, the appearance of such spectral regularity within a purely symbolic field theory invites deeper investigation.

17 C_{17} and the Emergence of Hadrons

The symbolic field $\psi_0 : M \to \{-1, +1\}$ admits increasingly complex local motif structures as its voxel support expands. While the 8-bit class $\mathcal{C}_8$ provides the foundational fixpoints for symbolic geometry, the 17-bit class $\mathcal{C}_{17}$

marks a structural threshold. Motifs in $\mathcal{C}_{17}$ possess sufficient internal structure to support internal symmetry constraints, directional activation, and structural subpartition. In this section, we define the canonical C_{17} motif structure and identify the minimal symbolic affordances that distinguish it from lower-dimensional motifs.

17.1 Canonical $\mathbf{C_{17}}$ Geometry

Let $\sigma \in \{-1, +1\}^{17}$ be a 17-bit motif. We fix a geometric embedding of the 17 voxel positions into three spatial layers, consistent with the Kepler-aligned configuration:

- **Layer $\mathbf{A_0}$** (voxels v_1–v_7): lower hexagonal ring with center
- **Layer B** (voxels v_8–v_{10}): central triangle
- **Layer $\mathbf{A_2}$** (voxels v_{11}–v_{17}): upper hexagonal ring with center

Each motif σ is then interpreted as a symbolic assignment to this spatial structure:

$$\sigma = (\sigma_1, \sigma_2, \ldots, \sigma_{17}) \in \{-1, +1\}^{17}$$

This structure supports nontrivial motif symmetry classes under the action of a geometric permutation group $G_{17} \subseteq S_{17}$ that preserves pairwise voxel distances and layer identity.

17.2 Symmetry Constraints and $\mathbf{D_3}$ Motifs

We define the middle-layer configuration of a motif as:

$$\sigma^{(B)} := (\sigma_8, \sigma_9, \sigma_{10}) \in \{-1, +1\}^3$$

A motif is said to be *D_3-positive* if $\sigma^{(B)} = (+1, +1, +1)$, and *$D_3$-negative* if $\sigma^{(B)} = (-1, -1, -1)$. These two classes exhibit maximal internal symmetry and rotational invariance about the motif's central axis. They form natural candidates for structurally stable configurations and are the focus of hadronic motif classification in the current work.

The full space $\mathcal{C}_{17}$ contains $2^{17} = 131{,}072$ motifs. Each distinct middle-layer configuration occurs in exactly $2^{14} = 16{,}384$ motifs, evenly partitioning motif space into symmetry strata.

17.3 Conditional Symmetry Expansion in C_{17} Motifs

Let $\sigma \in \{-1, +1\}^{17}$ be a symbolic motif defined on the Kepler-aligned C_{17} voxel configuration with canonical labeling $v_1, \ldots, v_{17}$. The voxel structure is partitioned into three layers:

- **Layer A_0** (voxels v_1–v_7): hexagonal ring + center at $z = 0$,
- **Layer B** (voxels v_8–v_{10}): central triangle at $z = h$,
- **Layer A_2** (voxels v_{11}–v_{17}): top layer, structurally identical to Layer A_0.

Definition 17.1 (Conditional Motif Symmetry Group)**.** Let $G_{17} \subseteq S_{17}$ be the full geometric symmetry group of the voxel layout (including all rigid permutations preserving pairwise distances). We define the *motif-conditional symmetry group* of σ as:

$$G_{17}(\sigma) := \{\pi \in G_{17} \mid \pi \cdot \sigma = \sigma\} \tag{139}$$

That is, $G_{17}(\sigma)$ consists of all geometric symmetries that *also* preserve the symbolic content of the motif.

Proposition 17.2 (Conditional Symmetry Expansion via Middle Layer Uniformity)**.** Let $\sigma^{(B)} := (\sigma(v_8), \sigma(v_9), \sigma(v_{10}))$ be the symbolic values of the middle layer. If

$$\sigma^{(B)} = (+1, +1, +1) \quad \text{or} \quad \sigma^{(B)} = (-1, -1, -1), \tag{140}$$

then the conditional symmetry group expands:

$$G_{17}(\sigma) \supsetneq G_{17}^{\text{base}}, \tag{141}$$

where G_{17}^{base} includes only rotations about the z-axis (e.g., C_6). In these uniform middle-layer cases, $G_{17}(\sigma)$ admits three additional rotational axes aligned with the legs of the triangle in Layer B.

Derivation. In the uniform middle-layer cases, the symbolic configuration of Layer B becomes invariant under all geometric symmetries of the triangle. Since Layer A_0 and Layer A_2 are structurally symmetric and located equidistant above and below Layer B, any rotation that permutes the triangle vertices while maintaining Layer A's structure becomes a valid symmetry of the full motif.

These additional axes correspond to C_2 or C_3 rotations through the triangle plane, allowing the A-layers to rotate as whole units about each leg of the triangle. This raises the symmetry group from the baseline (pure z-axis rotations) to an extended class containing multiple horizontal axes. □

17.4 Hadron Motif Dynamics

Definition 17.3 (Tag–Core Decomposition of Symbolic Hadrons)**.** Let $\sigma \in \mathcal{C}_{14}$ be a 14-bit symbolic motif. We define the **tag–core decomposition** as:

$$\sigma := \sigma_{\text{core}} \,\|\, \tau_{\text{tag}} \tag{142}$$

where: $\sigma_{\text{core}} \in \mathcal{C}_8$ is an 8-bit fixpoint motif selected from the canonical motif class of length 8; $\tau_{\text{tag}} \in \{-1, +1\}^6$ is a 6-bit symbolic tag; $\|$ denotes concatenation under motif binding constraints (e.g., local alignment, reflection, or curvature coupling).

Interpretation: The symbolic core defines the stable structural identity of the hadron—analogous to the quark flavor triple in a proton or neutron. The tag encodes charge asymmetry, binding state, and curvature alignment—analogous to color confinement and spin orientation. Changes in the tag can induce decay, isospin shift, or binding failure, enabling symbolic analogs of weak interaction channels.

Example 1 (Symbolic Proton Motif)**.** Let $\sigma_p \in \mathcal{C}_{14}$ be the 14-bit motif defined by:

$$\sigma_p := \sigma_{\text{core}} \,\|\, \tau_{\text{tag}} \tag{143}$$

with: $\sigma_{\text{core}} = (+1, +1, -1, -1, -1, +1, +1, -1)$ — a palindromic, moderately compressible fixpoint motif from $\mathcal{C}_8$; $\tau_{\text{tag}} = (+1, -1, +1, -1, +1, -1)$, a balanced, curvature-symmetric tag encoding stability and charge asymmetry.

Motif Metrics: $\psi_1(\sigma_p) = 3.00$ suggests moderate entropy; $\psi_2(\sigma_p) = 3.00$, relatively high compression; $s_{\text{sym}}(\sigma_p) = 1$, rotational asymmetry consistent with fermionic identity; CBD = 2, consistent with limited informational complexity.

Interpretation: The symbolic proton is a composite motif consisting of a symmetric 8-bit fixpoint (representing an up–up–down flavor triplet) and a curvature stable 6-bit tag encoding binding and charge asymmetry. The low entropy, moderate recursion, and highly regular tag of this informational

proton make it maximally persistent in symbolic curvature, capturing the extreme stability and charge structure of the physical proton.

Example 2 (Symbolic Neutron Motif)**.** Let $\sigma_n \in \mathcal{C}_{14}$ be the 14-bit motif defined as:

$$\sigma_n := \sigma_{\text{core}} \parallel \tau'_{\text{tag}} \tag{144}$$

with: $\sigma_{\text{core}} = (+1, +1, -1, -1, -1, +1, +1, -1)$ identical to the proton core; $\tau'_{\text{tag}} = (+1, +1, -1, -1, +1, -1)$ asymmetry introduced via two-bit tag.

Motif Metrics: $\psi_1(\sigma_n) = 4.00$, increased entropy, $\psi_2(\sigma_n) = 2.75$ — reduced compressibility, $s_{\text{sym}}(\sigma_n) = 1$ — same spin depth as proton, CBD = 3 — increased symbolic branching.

Interpretation: The symbolic neutron shares its core identity with the proton, but introduces curvature instability through tag asymmetry. The increased entropy and compression instability correspond to symbolic mass elevation and decay potential. This motif is a metastable informational structure, structurally predisposed to reentry or fragmentation—capturing the essence of neutron decay in symbolic curvature terms.

Proposition 17.4 (Symbolic Distinction Between Proton and Neutron)**.** Let $\sigma_p, \sigma_n \in \mathcal{C}_{14}$ be the symbolic proton and neutron motifs, each decomposed as:

$$\sigma_{p/n} = \sigma_{\text{core}} \parallel \tau_{\text{tag}}^{(p/n)} \tag{145}$$

with identical fixpoint core σ_{core} and tags $\tau_{\text{tag}}^{(p)}$, $\tau_{\text{tag}}^{(n)}$ differing by curvature-aligned bit structure.

Then: $\psi_1(\sigma_n) > \psi_1(\sigma_p)$; $\psi_2(\sigma_n) < \psi_2(\sigma_p)$; and $\mathcal{F}(\sigma_n) > \mathcal{F}(\sigma_p)$ at fixed temperature. The symbolic neutron based on ψ_0 dynamics emerges as a metastable motif prone to symbolic decay or reentry, whereas the proton is curvature stable under symbolic dynamics. Strikingly, these characteristics are consistent with known properties of QFT defined hadrons.

Interpretation: The proton and neutron differ not by structural identity but by the curvature alignment and the entropy cost of their tags. In IFT, symbolic decay is driven by entropy thresholds and compression loss, rather than external fields. The neutron becomes unstable when its tag deviates from curvature-preserving alignment.

17.5 Nontrivial Affordances

Motifs in $\mathcal{C}_{17}$ are the first to admit nontrivial internal substructure. They contain enough bits to encode *distinct internal zones*—such as axial cores and peripheral rings. They support stable layer-wise assignments: center, ring, triangle. They preserve global motif identity under restricted symmetry groups $G_{17}(\sigma)$ while allowing local asymmetry.

These properties allow motifs in $\mathcal{C}_{17}$ to exhibit behaviors not accessible to 8-bit motifs. In particular, the symbolic motifs in $\mathcal{C}_{17}$ possess the internal complexity to support novel structural advantages:

1. **State Register:** Internal voxel configurations may stably encode finite symbolic states.
2. **Symbol Alphabet:** Outer-ring voxel sequences may encode recurring motif classes or symbolic tokens.
3. **Conditional Branching:** Asymmetries across the motif structure may enable logical differentiation.
4. **Transition Logic:** Mappings between motifs under local perturbation may encode symbolic evolution.

While suggestive, no computational interpretation is imposed here. These affordances are geometric and structural. They reflect the symbolic capacity of C_{17} motifs, but do not prescribe behavior.

18 Conclusion

SSFT begins with a minimal assumption: a binary scalar field $\psi_0 : M \to \{-1, +1\}$ defined over a smooth manifold M. From this field, symbolic motifs emerge as invariant structures, classified into canonical sets such as $\mathcal{C}_8$ and $\mathcal{C}_{17}$. These motifs are not analogs of particles; they are definitional fixpoints, i.e. irreducible entities that instantiate physical identity through symbolic contrast. Postulating such fundamental entities is not a new idea. Leucippus (c. 500 BCE) and Democritus (c. 460 – c.370 BCE) would immediately recognize motifs as *"atoms."*

From motif-level structure, SSFT constructs directional fields (ψ_1), activation profiles (ψ_2), and a symbolic metric $G_{\mu\nu}$—each derived without postulates of energy, geometry, or symmetry. Curvature is encoded not as deformation of a background but as projection from motif asymmetry and activation density. Identity is not local; it is absolute. Motion arises not from force, but from entropy gradients and activation geometry.

The framework supports a symbolic analog of Einstein's field equations, encodes particle identity through motif multiplicity, and aligns symbolic Laplacians with the spectral structure of number theory. Without invoking quantum amplitude or spacetime dynamics, SSFT reproduces key features of field interaction: symmetry-breaking, charge quantization, gauge invariance, and spectral discreteness.

No physical claims are made. The field ψ_0 remains an unobserved construct. Yet its structure admits interpretation. From discrete symbols, which are minimally defined and fully invariant, emerge fields, curvature, and higher order structure. Whether this scaffolding supports physics remains an open question. But as a self-contained system of symbolic dynamics and motif geometry, SSFT offers a coherent, derivational framework with testable internal consequences and a precise mathematical identity.

19 Methods

Colab, Overleaf, and a custom OpenAI GPT 4o large language model (LLM) were used in the writing of the manuscript. The LLM was used predominantly help with mathematical equations and with python coding. The text was written entirely by the author who assumes all responsibility for any errors or inaccuracies.

Acknowledgments and Dedication

This work was carried out entirely without the support of grant funding, institutional infrastructure or resources of any kind. This work could not have been done without extensive discussion and kind feedback from Melissa Bates, Brad Fels, and Erik Tomasson.

Dedication

This paper is dedicated to the memory of Charles Joseph "Charlie" Bates. Charlie possessed a joyful, loving, and clear-eyed intelligence that captivated everyone he met. I tried, however feebly, to infuse this work with his spirit. I imagine Charlie as the student who would have raised his hand in physics seminar and said with astonishing self-confidence and radical candor:

"Professor, I think you are wrong."

QFT Term	SSFT Status	SSFT Semantic Equivalent
Elementary particle	Defined	Defined via motif class P_σ; see electron.
Field amplitude	Discarded	Replaced by ψ_2 activation; no scalar field amplitude exists in SSFT.
Inner product	Defined	Reframed as motif support metric in H_Σ; see inner product.
Wavefunction $\psi(x)$	Discarded	No equivalent scalar function; symbolic field ψ_0 replaces it.
Probability density	Defined	Modeled via activation envelope $A[\sigma]$ and recurrence.
Born Rule	Reframed	Defined using entropy-based distributions; see entropy.
Charge	Defined	Topological and transport-based; see charge.
Mass	Defined	Defined by ψ_1-induced curvature; see mass.
Energy	Defined	Defined over motifs via symbolic energy functional; see energy.
Entropy	Defined	Derived from motif gradients; see entropy.
Superposition	Retained	Linear combinations of motif modes in H_Σ; see superposition.
Gauge theory	Defined	Symbolic $U(1)$ fields constructed from ψ_2; see gauge theory.
Noether's Theorem	Retained	Motif-preserving diffeomorphisms yield conservation laws; see Noether's Theorem.
Path integral	Deferred	Not defined; motif Laplacians may offer a spectral analog.
Fock space	Deferred	No symbolic creation/annihilation operators currently defined.
Renormalization	Deferred	No divergence structure or running constants defined in SSFT.
Coherence	Discarded	Semantically vague; excluded from SSFT vocabulary.

Table 3: Semantic comparison of QFT and SSFT terminology with token discipline.

20 Citations INCOMPLETE: .bibtex under construction

References

[1] Shannon, C. E. (1948). A Mathematical Theory of Communication. *Bell System Technical Journal*, **27**, 379–423, 623–656.

[2] Cover, T. M., & Thomas, J. A. (2006). *Elements of Information Theory* (2nd ed.). Wiley-Interscience.

[3] Kieffer, J., & Cover, T. M. (1994). Review: The Noisy-Channel Coding Theorem in Chapters 8–10. *SIAM Review*.

[4] Wikipedia Contributors. (2025). *Shannon–Hartley Theorem*. Retrieved from `https://en.wikipedia.org/wiki/Shannon-Hartley_theorem`

[5] Wikipedia Contributors. (2025). *Binary Symmetric Channel*. Retrieved from `https://en.wikipedia.org/wiki/Binary_symmetric_channel`

[6] Marton, K. (2013). An inequality for relative entropy and logarithmic Sobolev inequalities in Euclidean spaces. *Journal of Functional Analysis*, **264**(1), 34–61.

[7] Marton, K. (2013). Logarithmic Sobolev inequalities in discrete product spaces. *Combinatorics, Probability & Computing*.

[8] Burnside, W. (1897). On the theory of groups of finite order. *Proceedings of the London Mathematical Society*, **s1-28**(1), 162–189.

[9] Li, M., & Vitányi, P. (2008). *An Introduction to Kolmogorov Complexity and Its Applications* (3rd ed.). Springer.

[10] Grünwald, P. D. (2007). *The Minimum Description Length Principle*. MIT Press.

[11] Einstein, A. (1915). Die Feldgleichungen der Gravitation. *Sitzungsberichte der Preussischen Akademie der Wissenschaften zu Berlin*, 844–847.

[12] Wald, R. M. (1984). *General Relativity*. University of Chicago Press.

[13] Carroll, S. M. (2004). *Spacetime and Geometry: An Introduction to General Relativity*. Addison-Wesley.

[14] Yakaboylu, E. (2024). Hilbert–Pólya Hamiltonian construction with self-adjoint similarity transform. *arXiv preprint* arXiv:2405.00205.

[15] Bender, C. M., Brody, D. C., & Müller, M. P. (2017). Riemann zeros and the xp Hamiltonian. *Physical Review Letters*, **118**(13), 130201.

[16] Connes, A. (1999). Trace formula in noncommutative geometry and the zeros of the Riemann zeta function. *Selecta Mathematica*, **5**(1), 29–106.

[17] P. Galison and A. Manohar, "Two Z's or not two Z's?", *Phys. Lett. B* **136** (1984) 279–283.

[18] B. Holdom, "Two U(1)'s and ϵ charge shifts", *Phys. Lett. B* **166** (1986) 196–198.

[19] R. Essig, J. A. Jaros, W. Wester et al., "Dark Sectors and New, Light, Weakly-Coupled Particles", arXiv:1311.0029 [hep-ph] (2013).

[20] F. Curciarello, "Review on Dark Photon searches", *Acta Phys. Polon. B* **47** (2016) 1329–1338.